

## **Spatially Variable Legacy Effects of Rainfall Extremes on High Arctic Shrub Growth**

Rúna Í. Magnússon<sup>1</sup>, Taoran Chen<sup>1</sup>, Manon van den Dolder<sup>1</sup>, Julian Michiels<sup>1</sup>, Tosca Koeze<sup>1</sup>, Mathieu Decuyper<sup>2</sup>, Simone I. Lang<sup>3</sup> & Juul Limpens<sup>1</sup>

- 1) Plant Ecology & Nature Conservation Group, Wageningen University & Research, Droevendaalsesteeg 3a, 6708PB Wageningen, the Netherlands
- 2) Forest Ecology & Management Group, Wageningen University & Research, Droevendaalsesteeg 3a, 6708PB Wageningen, the Netherlands
- 3) Department of Arctic Biology, the University Centre in Svalbard, P.O. Box 156, N-9171 Longyearbyen, Svalbard, Norway

## Introduction

Arctic tundra ecosystems are undergoing fundamental change, with a warming trend three to four times faster than the global average (AMAP, 2025, Rantanen et al., 2022), increases in various extreme events (AMAP, 2025) and, more recently, reductions in carbon sink strength (See et al., 2024). Beside temperature change, climate reanalysis data for the Arctic (> 65°N) shows increases in precipitation of 2% - 10% over the period 1979-2023 (AMAP, 2025). Larger proportional increases in rainfall are reported (e.g. 25% increase over 1971-2019) (AMAP, 2021), due to a general shift from precipitation as snow to precipitation as rain in a warmer Arctic (AMAP, 2025, Dou et al., 2022, Bintanja and Andry, 2017). Observed and predicted increases in year-to-year variability of rainfall, suggest that the Arctic will continue to show both extreme summer rainfall episodes and drought spells (Wang et al., 2021, AMAP, 2025, Bintanja et al., 2020). However, the impact of rainfall extremes on Arctic ecosystems is understudied compared to that of warming.

Since the late 1990s, satellite records of the polar regions show that the Arctic is “greening” (Frost et al., 2025). Both space-borne and field-based observations find that Arctic vegetation is becoming taller and more productive, with particularly strong increases in shrubs (Mekonnen et al., 2021, Berner et al., 2020, Henry et al., 2022, Bjorkman et al., 2018, Elmendorf et al., 2012a, Elmendorf et al., 2012b). This affects the functioning and carbon balance of Arctic ecosystems (Schuur et al., 2022, Chen et al., 2024, Myers-Smith et al., 2019) and results in locally heterogeneous feedbacks to other ecosystem components, such as permafrost (Heijmans et al., 2022, Lorantý et al., 2018), the diversity and abundance of other plant groups (e.g. cryptogams) and resource availability for herbivores and pollinators (Henry et al., 2022, Fauchald et al., 2017, Prevéy et al., 2019).

Out of various tundra plant functional groups, shrubs tend to show strongly positive responses to warming, although the degree of response varies with local moisture status, baseline climate and shrub growth form (Myers-Smith et al., 2015a, Elmendorf et al., 2012a, Elmendorf et al., 2012b). Many Arctic shrub species form small yet distinguishable tree-rings, with larger tree-rings indicating higher growth and biomass accretion in that year (Myers-Smith et al., 2015b), and as a result, tree-ring studies on Arctic shrubs have been essential in understanding local contrasts in temperature sensitivity (Buchwal et al., 2020, Myers-Smith et al., 2015a). Recent evidence has highlighted the role of increasing climatic variability, potential non-linearities in climate-growth associations (Magnússon et al., 2023, Francon et al., 2020), sea-ice dynamics (Buchwal et al., 2020) and particularly moisture availability (Buchwal et al., 2020, Gamm et al., 2018, Ackerman et al., 2017, Myers-Smith et al., 2015a) as important factors regulating shrubs’ warming response. This suggests that expected future changes to Arctic rainfall dynamics, and their implications for moisture availability, will significantly shape future Arctic shrub dynamics.

Moreover, tree ring studies conducted in the North-Eastern Siberian lowland tundra found that shrub growth showed significant associations with rainfall dynamics in the preceding growing season (Magnússon et al., 2023, Blok et al., 2011), suggesting that impacts of future precipitation and drought extremes may not be limited to a single season. Arctic shrubs have additionally been demonstrated to adapt their relative investment in above- and belowground tissues under climatic variability (Buchwal et al., 2013, Myers-Smith et al., 2015b). Variability in within-shrub resource allocation and carry-over effects under

precipitation extremes are, however, rarely considered in studies of climate-sensitivity of Arctic shrubs.

As global warming induces multiple simultaneous trends and extreme events in Arctic weather systems, it is becoming increasingly difficult to ascribe annual shrub growth dynamics to any single manifestation of climate change. This illustrates the limitations of conventional correlative climate-growth studies and the need for targeted experimental evidence. Previous studies have successfully quantified wood growth, bark investment and wood vessel properties of various shrub species in climate manipulation set-ups (Power et al., 2024, Iturrate-Garcia et al., 2017). Moreover, annual dynamics of tree-ring widths can provide reliable proxies for aboveground biomass (Le Moullec et al., 2019) and ecosystem level gross primary productivity (Tei et al., 2019). Hence, applying tree-ring-based studies in an experimental context provides a compelling strategy to provide causal evidence of the impact of various future climate extremes on Arctic shrub growth.

Here we study the effects of experimental heavy rainfall events at various landscape positions and various seasonal timings on the radial growth of the High Arctic dwarf shrub *Salix polaris* on Svalbard. *S. polaris* is a keystone species in Svalbard ecosystems that represents a large share of the total vascular plant biomass and of the diet of herbivores (Nakatsubo et al., 2010, Bjørkvoll et al., 2009). We studied (i) how heavy rainfall events in summer affect shrub radial growth in contrasting climate zones and soils on the archipelago. We explicitly evaluated whether these impacts differ among (ii) early and late summer rainfall events, and (iii) between plant roots and shoots. Finally, we evaluate whether (v) legacy effects manifest in the summers after experimental treatment. We thereby deliver causal insight into the effect of predicted increases in heavy rainfall events on Svalbard (Hanssen-Bauer et al., 2019) on the growth of a keystone shrub species, with important consequences for the future functioning of High Arctic ecosystems. Lastly, we provide proxy records of shrub growth for several ecosystems on Svalbard for recent decades, and new insight into its current climatic drivers in this rapidly changing environment.

## Methods

### Study System

We experimentally evaluated the impact of heavy rainfall events in summer on shrub growth in several sites on the High Arctic archipelago of Svalbard. Svalbard is warming circa seven times faster than the global average (Nordli et al., 2020) and has seen record-breaking summer temperatures over the course of our experiment, specifically in 2022-2024 (van den Broek et al., 2025), making this one of the most rapidly warming regions on Earth (AMAP, 2025). MODIS satellite records of vegetation “greenness” suggest that local vegetation communities responded with increased productivity and growing season duration (Karlsen et al., 2024). Furthermore, Svalbard and the North Atlantic Arctic region have shown strong increases in total precipitation and rainfall in recent decades in reanalysis datasets (AMAP, 2021), with increased occurrence of heavy rainfall events. Such extreme events are expected to occur increasingly under continued warming (Hanssen-Bauer et al., 2019).

Study sites for rainfall manipulation were set up from 2022 to 2024 in Adventdalen, Endalen (two locations each) and Ny-Alesund (one location). Sites were selected to represent a variety of soil types (mineral vs. organic soils in Adventdalen), topography (flat vs. sloping topography in Adventdalen and Endalen), tundra climatic subzones (C for Adventdalen and Endalen, B for Ny-Alesund) (CAVMTeam, 2003, Elvebakk, 1999) and plant communities. All experimental plots contained *S. polaris* shrubs. Site conditions are summarized in Table 1 and described more extensively in Magnússon et al. (2024).

Table 1. Description of study sites. Adapted from Magnússon et al. (2024).

Site	Coordinates	Landform	Soil Description	Vegetation Description
1 - Adventdalen - Loess Terrace	78.199°N , 15.844°E	Loess terrace (Strand et al., 2021). Predominantly flat terrain	Mineral, 2.5 m deposit of silt to fine-grained sand (Strand et al., 2021).	Sparse cover of <i>Salix polaris</i> , <i>Polytrichum sp.</i> moss, <i>Bistorta vivipara</i> , <i>Poa arctica subs. arctica</i> , <i>Festuca rubra subs. richardsonii</i> , <i>Alopecurus ovatus</i> . Cryptogamic and saline crusts locally.
2 - Adventdalen - Polygonal Tundra	78.192°N , 15.862°E	High center polygons. Predominantly flat terrain, microtopographical gradients of polygon troughs and centers	> 30 cm of predominantly organic soil, with gradual transition to finer mineral sediment	Dense cover <i>Calamagrostis neglecta subs. groenlandica</i> , <i>Dupontia fisherii</i> , <i>Carex subspathaceae</i> , <i>Salix polaris</i> , <i>Bistorta vivipara</i> and various bryophytes.
3 - Endalen - River Terrace	78.185°N , 15.767°E	River terrace. Predominantly flat, gentle gradient from footslope (snowbed) to bank of river bed (snow free earlier)	Gravelly to fine mineral sediment overlain by organic layer and moss layer of variable thickness	Dense cover of bryophytes (predominantly <i>Sanionia uncinata</i> ), <i>Salix polaris</i> , <i>Bistorta vivipara</i> , <i>Poa arctica subs. arctica</i> , <i>Festuca rubra subs. richardsonii</i> , <i>Alopecurus ovatus</i> .
4 - Endalen - Slope	78.184°N , 15.766°E	North-facing Slope. Slope angle of $\pm 9^\circ$ or 15 %. Variable microtopography and hydrology.	Gravelly to fine mineral sediment overlain by organic layer and moss layer of variable thickness	Dense cover of various bryophytes (variable thickness), <i>Salix polaris</i> , <i>Bistorta vivipara</i> , <i>Poa arctica subs. arctica</i> , <i>Festuca rubra subs. richardsonii</i> , <i>Luzula confusa</i> , <i>Alopecurus ovatus</i> . Locally cryptogamic crusts, <i>Cassiope tetragona</i> and <i>Dryas octopetala</i> .
5 - Ny-Ålesund - Westbyelva	78.920°N , 11.917°E	Terrace. Predominantly flat, gentle gradient towards Westbyelva	Weathered bedrock overlain by shallow layer of coal dust (former mine area) and organic layer	Cryptogamic crusts, sparse cover of <i>Salix polaris</i> , <i>Luzula confusa</i> , few forbs, mosses. Locally dense <i>Racomitrium</i> cover.

## Experimental Design

We tested the impacts of heavy rainfall events in summer by irrigating 4m diameter circular plots with 50mm additional rainfall (an approximate doubling of average June-August precipitation), at different seasonal timings in 2022 and 2023. In each of the five sites (Table 2) we assigned 6 (Ny-Alesund, Endalen) or 7 (Adventdalen) control (C) plots, and selected irrigated plots with roughly similar microtopography and plant communities. During a first experiment, we supplied 50mm additional rainfall in individual sessions of 10mm with three days in between during late summer 2022 (July 22nd to August 6th) in irrigated (I) plots with the same replication of 6 or 7 plots per site. The amount of 10mm per treatment was set to mimic a natural extreme rainfall event, based on recent meteorological observations at Svalbard Airport (Magnússon et al., 2024, NCCS, 2025). In 2023, we set out two additional treatments with the same amount of replications and similar plot conditions, in which we supplied a similar rainfall treatment (50mm total in sessions of 10mm) in early summer (June 15th - 27th) or late summer (July 1st to 13th). These are referred to as E and L plots, and test the role of seasonal timing of heavy rainfall events in affecting shrub growth. At the site in Ny-Alesund, the E and L treatments in 2023 were supplied at later seasonal timing (July 5th to 16th and July 20th to 30th, respectively) due to later snowmelt. In order to capture legacy effects on growth of the I treatment in 2023 and 2024, and of the E and L treatment in 2024, we harvested shrubs after the peak growing season in 2024 (early to mid August). Shrubs were only harvested from sites 1, 2, 4 and 5 (Table 1), as irrigation treatment was discontinued in the third site due to damaged plots and lack of space for new E and L treatment plots (Magnússon et al., 2024).

Water was supplied from local surface water bodies, fed by snowmelt and potentially to some extent by groundwater and melting of active layer ice. We compared the chemical composition of the irrigation water with locally collected rainfall samples and wet deposition values measured in Ny-Alesund (Table S1), and found no indications of nutrient addition resulting from our treatment compared to the additions effectuated by natural rainfall and wet deposition (Table S2). Since the irrigation treatment did not result in substantial effects on permafrost thaw and soil temperatures either (Magnússon et al., 2024), we do not expect any confounding effects from soil warming or cooling, or fertilization as a result of our watering experiment. Lastly, plots were set out at least 5m apart, and in sloping sites we did not set up irrigated plots directly upslope of plots belonging to other treatments, to reduce potential spillover effects. Treatment plots consisted of a 4m diameter circle, in which regular monitoring measurements were performed in 2022-2024 at nine fixed points along the inner perimeter (1.5m from plot centre) and centre of each plot (Magnússon et al., 2024).

## Focus Species

One of Svalbard's most widespread species is the tree-ring forming dwarf shrub *Salix polaris*, which has known potential as a proxy for annual shrub growth and biomass (Le Moullec et al., 2019, Le Moullec et al., 2020, Buchwal et al., 2013). *S. polaris* has a circum-arctic distribution (Le Moullec et al., 2019) and is a prostrate shrub with a mat-forming growth form. Its branches predominantly grow belowground and in the moss layer, with shoots of several centimeters extending aboveground. It is common throughout a wide range of landscape positions and soil types on Svalbard (Elven et al., 2020). From the root collar, it

generally forms a strongly branched belowground structure of stems, and a core root with several lateral roots (Elven et al., 2020, Le Moullec et al., 2019). In moist tundra meadows with denser vegetation, its growth form can be more complex with extensively branched and interconnected belowground structures (Le Moullec et al., 2019). Sexual reproduction is predominantly wind-dispersed, and asexual reproduction occurs through belowground shoots (Elven et al., 2020). Stems can reach a thickness of up to around 0.5 to 1 cm (several mm excluding bark) at the root collar (the oldest part of the shrub) (Le Moullec et al., 2019). Individuals typically reach ages of several decades (Le Moullec et al., 2019, Buchwal et al., 2013, Le Moullec et al., 2020) and form tree-rings with a mean width of around 0.14 - 0.04 millimeters (Le Moullec et al., 2019, Buchwal et al., 2013, Opała-Owczarek et al., 2018).

### Shrub Sampling Strategy

We sampled two shrub replicates from each experimental plot for Locations 1, 2, 4 and 5, leading to a total of 208 shrubs from 104 plots. We carefully dug out belowground parts of individual shrubs, identifying the root collar as a thicker, often strongly bent part of the stem, from which shoots usually branch out laterally. We cut 2 cm segments from the root collar, a root, a belowground shoot and an aboveground shoot (shoot end) for each shrub, which were stored individually in 2mL eppendorf vials with a 1:3 mixture of vodka and glycerol to prevent bacterial and fungal growth and desiccation. Since we sampled from the perimeter of a treated area, and wanted to obtain a representative selection of the local shrub population, it was both impossible and unwanted to select larger individuals, as is common practice in polar shrub dendrochronological studies (Myers-Smith et al., 2015b). However, visually damaged individuals or individuals with very unclear transitions from root to shoot system were discarded and replaced during sampling.

### Sample Processing, Tree-ring Measurement & Series Detrending

An elaborate workflow for tree-ring sample preparation, measurement, cross-dating and detrending is available in Text S1. Key steps are summarized below.

± 20 µm thin sections were cut with a GSL1 sledge microtome (WSL, Birmensdorf, Switzerland) (Gärtner et al., 2014) perpendicular to the axis of elongation of each shrub segment. Each section was visually inspected under a microscope and sectioning was repeated if necessary. Samples were stained using a safranin/astra blue mixture (Gärtner and Schweingruber, 2013) to enhance visual contrasts between various wood tissues, and rinsed with demi water and ethanol solutions of increasing purity. Samples were then embedded in resin on glass slides and photographed and digitized using a camera microscope. Images with camera-calibrated scale bar and dpi settings were exported at 4000 by 3000 pixel resolution using LAS X version 4.13 (Leica Microsystems, Wetzlar, Germany), and multiple images at higher magnification were stitched together if needed for larger samples.

We applied a serial sectioning and hierarchical crossdating approach to measure tree-ring widths (Hallinger et al., 2010, Wilmking et al., 2012), consecutively measuring and cross-dating among three radii per section and four sections per shrub in Coorecorder version 9.0

(Cybis, Saltsjöbaden, Sweden). Serial sectioning of segments - including the root collar - maximizes the number of tree-rings and certainty of measurement obtained from a sample, and allows to account for variability in resource allocation within and across sections (Kolischuk, 1990, Myers-Smith et al., 2015b, Buchwal et al., 2013). After initial (unbiased) measurement, we used reference series from earlier studies (Le Moullec et al., 2020) and half-chronologies based on averaged ring-widths of easily discernible samples for each site (see Text S2). After inspection for missing rings, radii per segment were averaged in CDendro version 9.0 (Cybis, Saltsjöbaden, Sweden). In many cases, however, the above-ground shoot-end was not considered further due to an insufficient number (5 or less) of rings. In case a shrub showed extensive damage, poorly discernible rings or poor visual fit to the site reference series, we discarded the measurements and cut either new sections from the same 2cm shrub fragments, or continued with the second sample for the same plot.

Individual section-averaged tree-ring series were combined per experimental site (Table 1) and exported as Tucson format (.rwl) decadal files. A final round of visual checks for missing rings and within-shrub and among-shrub fits was performed in WinTSAP v. 4.70d (Rinntech, 2017) and samples were revisited and checked for missing rings if necessary. Tree-ring datasets were then detrended and inspected using the dplR package (Bunn, 2008) in R version 4.4.1. We removed age-related trends using an age-dependent cubic smoothing spline with an initial stiffness of 20 years and a restricted slope (zero) at the end of the series (Bunn, 2008, Cook and Kairiukstis, 1990, Melvin, 2004). Raw series were detrended by division against fitted values and interseries correlation was computed according to Briffa and Jones (1990). We corrected for temporal autocorrelation (“pre-whitening”) using a first-order autoregression function. We then exported age-detrended and pre-whitened residual RWI values at the section-level, shrub-level (averages of all segments within a shrub) and site-level (site chronology, average of all shrubs within a site). For the site chronologies, we used a residual chronology with a minimum sample depth of three individuals. We also removed the RWI values of all experimentally treated plots (I plots from 2022 onwards, E and L plots from 2023 onwards) to obtain site-level chronologies of shrub radial growth under baseline conditions. We did not make separate root, root collar and shoot chronologies due to limited series length root and particularly shoot samples.

### Weather Data

We downloaded monthly average temperature and total precipitation for the Svalbard Airport (station SN99840) and Ny-Alesund (station SN99910) meteorological stations from [seklima.met.no](https://seklima.met.no) (Norwegian Meteorological Institute) (NCCS, 2025) available from 1975 onwards. The Svalbard Airport data were used for the Adventdalen and Endalen tree-ring data (< 10km from sites), and the Ny-Alesund record for the Ny-Alesund tree ring data (< 500m from site). Yearly dynamics of seasonal (JJA, SON, DJF, MAM) temperature averages and precipitation sums are available in Fig. S6. We obtained seasonally averaged snow depth measurements for the same stations (available since 2008 for Svalbard Airport and 2009 for Ny-Alesund) and rain-on-snow sums calculated according to Vickers et al. (2022) (Fig. S7). The Svalbard Airport precipitation record shows six months of missing data in 2021 (May-August, October-November) which were gap-filled using a linear fit against monthly rainfall totals of the nearest available station (Isfjord Radio, station SN99790, LOOCV-RMSE of monthly rainfall totals over 2020 - 2025 = 10.23mm). During our

experimental treatment and in the year directly following (2022-2024), JJA (June-August) temperatures were 7.7°C (2022), 7.4°C (2023) and 8.5°C (2024) at Svalbard Airport, compared to a multidecadal mean of 5.6°C (1992-2021). JJA temperatures in Ny-Ålesund were 6.1°C (2022), 5.9°C (2023) and 7.0°C (2024), compared to a multidecadal mean of 4.4°C (1992-2021) (Fig. S6a).

## Statistical Evaluation

### *Baseline Climate-Growth Associations*

To assess each site's baseline climate-growth relations, we compared residual chronology ring-width indices (excluding observations from treated plots in 2022-2024) to the monthly average temperature and total precipitation values. We calculated spearman correlation values per individual month with standard bootstrapped ( $n = 1000$ ) 95% confidence intervals using the treeclim R package (Zang and Biondi, 2015). We generated correlation values for the months ranging from October previous year to August current year, since we expected that preceding winter conditions may affect growth in summer, and *S. polaris* is generally observed to go into senescence in August. Although the limited length of our growth chronologies prevented the selection of a wider range of months to test against, we were specifically interested in potential lagged effects of conditions in previous summers (Blok et al., 2011, Magnússon et al., 2023). Hence, we additionally computed bootstrapped 95% CI's for seasonally aggregated climate variables, ranging from previous summer (pJJA), preceding autumn (SON), preceding winter (DJF), spring (MAM) and summer (JJA).

Since the overlap between snow depth and rain-on-snow datasets and tree-ring chronologies was only 14 or 15 years, we conducted a simple partial correlation analysis of Spearman correlation values for associations between baseline site level RWI (chronology) and seasonal snow depth and rain-on-snow for the pJJA, SON, DJF, MAM and JJA seasons as well as total snow season (S-M) rain-on-snow. For each location, we used average temperature during the site-specific observed main period of climate sensitivity in summer (e.g. June-July) as a controlling variable for partial correlation analysis.

### *Effects of Experimental Rainfall*

To test whether experimental rainfall addition (+ 50mm) induced differences in shrub radial growth, we extracted shrub-averaged ring-width indices (after detrending and removal of first-order temporal autocorrelation) and used linear mixed effects models to evaluate whether radial growth (RWI) differed among treatment classes (C, I, E, L) in the years during, following and prior to experimental intervention. We selected a common period of 2018 to 2024 across experimental locations to ensure a valid comparison, since the youngest shrub dated from 2017 (the ring width value for 2017 is lost after correcting for first-order autocorrelation).

We first compared ages among treatment groups per location using a one-way ANOVA, to rule out confounding effects of different age composition among treatment classes. We then used a linear mixed effects model per individual location with RWI as a response, and factors "year", "treatment" and their interaction as fixed effects. We added a random intercept for each unique shrub to account for repeated measurement on the same individual, and potential shrub- or plot-level long-term deviations in growth. We then repeated the analysis above at the level of individual sections. Since the above ground shoot

end sections were often omitted due to insufficient rings, we restricted this analysis to the root, root collar and shoot sections. We used a similar random effects structure and extended the fixed structure of the LMM with up to three-way interactions for the factors “section”, “year” and “treatment”, to test whether the experimental rainfall additions had had diverging effects on above- or belowground growth and resource allocation.

For all LMM's, we used the lme4 package (Bates et al., 2024) to construct models. We used the lmerTest package (Kuznetsova et al., 2024) to generate Type III ANOVA tables, with p values for individual terms based on F-tests. We visually checked the residuals of our models for normal distribution using histograms and QQ-plots, and for heteroscedasticity using scatterplots of residuals against fitted values. We tested the null hypothesis that RWI values showed consistent values across treatments across all years (since we hypothesized that RWI among treatments are similar prior to the treatment, but diverge after 2022 or 2023) based on the significance of the treatment:year interaction term. In case of a significant interaction term, we performed a post-hoc test using the emmeans package (Lenth, 2024), by evaluating the significance of pairwise differences among treatments for each specific year. We used a multivariate normal correction to correct p values for multiple testing (Lenth, 2024). For the section-level RWI dataset, we tested the null hypothesis that RWI values showed consistent values across treatments across all sections and years (alternatively, RWI among treatments are similar prior to the treatment, but diverge after 2022 or 2023, with variable responses in different section types) based on the significance of the treatment:year:section interaction term. If significant, we followed up with a similar post-hoc test, with pairwise differences per year, per section type. Throughout all statistical analysis we use a significance criterium of  $\alpha = 0.05$ , and p values under 0.01 are reported as tendencies.

## Results

### Sample Measurement and Cross-dating

Out of four sampled locations, we only managed to accurately measure and crossdate sufficient shrubs for two locations (Location 2 - Adventdalen, Polygonal Tundra and Location 5 - Ny-Alesund, Westbyelva). For the other two sites, measurement and evaluation was discontinued due to high prevalence of damaged, unmeasurable shrubs and unreliable half-chronologies (Table S3). The remaining two sites showed sufficient visual correlation among series selected for a half-chronology, and with pre-existing ring-width series (Le Moullec et al., 2020), and the reference chronology developed for Endalen (Text S2, Fig. S2, Table S4). For Location 2 and 5, about one half to two thirds of the samples could be successfully crossdated, and with a back-up sample available this resulted in datasets of 24 and 23 shrubs, respectively. All sites had at least five (1 plots, Location 5), and in all other cases six cross-dated shrubs per treatment. No significant differences were found in shrub age among the treatment classes at either site (Table S5, S6, one-way ANOVA,  $p > 0.05$ ).

### Site Chronologies

The site chronologies for the two successfully cross-dated sample sets show similar peaks in 2022 and dips in 2008 and 2021 (Fig. 1), which stand out as particularly warm and cold summer seasons (Fig. S6a). Interseries correlations for the dataset with all sections were 0.49 (Location 5) and 0.43 (Location 2), which we consider reliable and realistic for *S. polaris* (Buchwal et al., 2013, Opała-Owczarek et al., 2018, Owczarek et al., 2020), especially given the difficulty of the material and the fact that we adopted a relatively unbiased sampling approach. Our samples show a relatively small average tree ring width 0.034 - 0.039 mm) and age range (usually under 20 years). Further statistical details of the two chronologies are presented in Table 2.

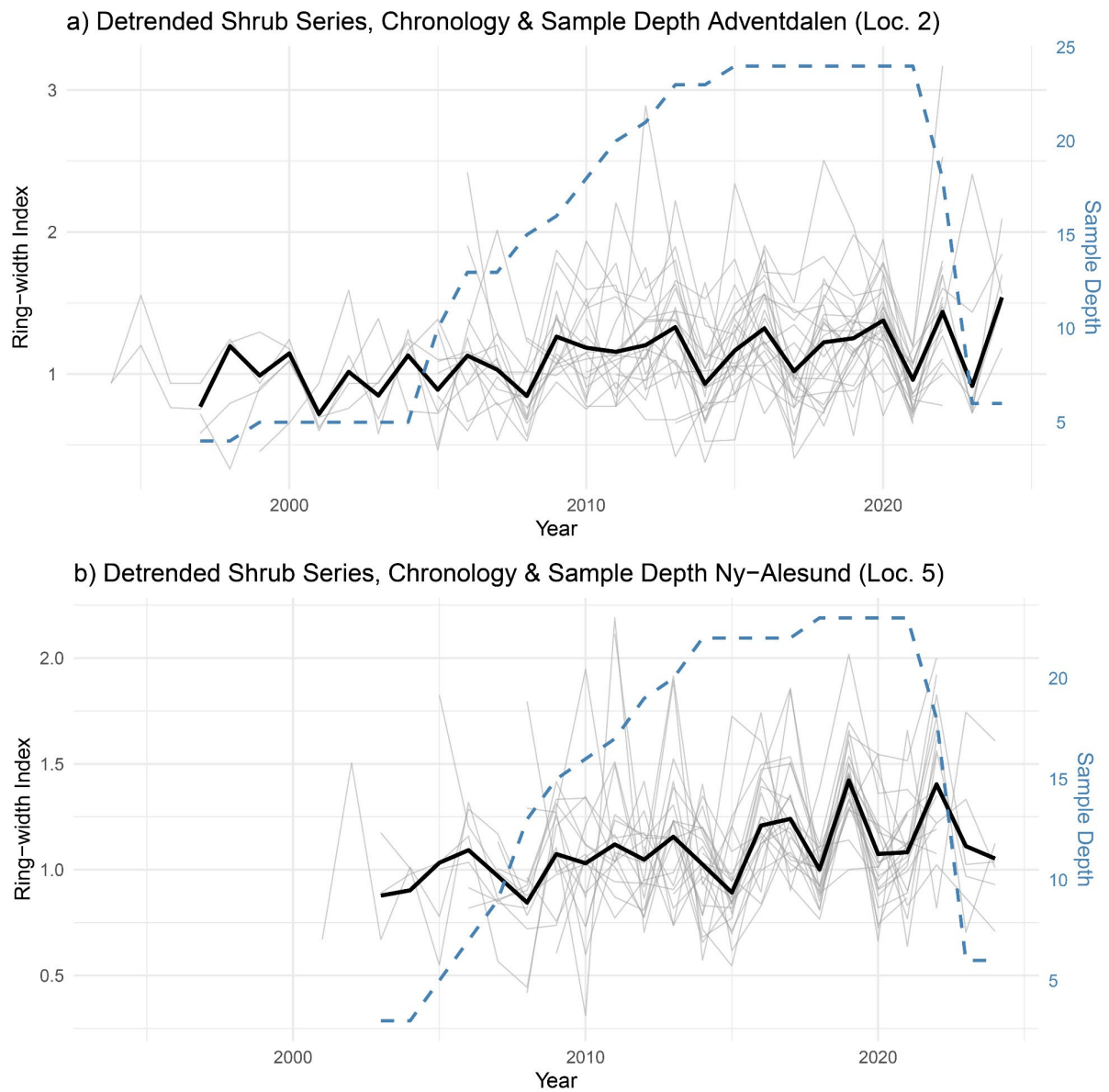


**Figure 1)** Site Ring-Width Index (RWI) chronologies for **a)** Location 2 (Adventdalen, Polygonal Tundra) and **b)** Location 5 (Ny-Alesund, Westbyelva). Dashed blue lines indicate sample depth (number of shrubs) per year. Grey lines indicate shrub-averaged (multiple sections) age-dependent spline detrended and pre-whitened (1st order autoregression model) RWI of individual shrubs. Thicker black lines indicate site chronology, with a minimum sample depth of 3.

Table 2) Site Chronology Statistics - at the level of Shrub Averaged Growth Series

Site	Nr. Shrubs	Time Span <sup>1</sup>	Mean Interseries Correlation <sup>2</sup>	Mean Sensitivity <sup>3</sup>	AR(1)	Mean ring width (mm)	Mean Age	St. dev. Age
2	24	1997 (1994) - 2024	0.49	0.36	-0.04	0.034	18.38	5.90
5	23	2003 (2001) - 2024	0.43	0.32	-0.13	0.039	15.87	3.90

- 1) Starting year indicates first year with sample depth of 3 or more series, while the number in brackets indicates oldest observed tree-ring (see Fig. 1)
- 2) Following Cook et al. (1990)
- 3) Following Biondi and Qeadan (2008)

### Baseline Climate-Growth Associations

Bootstrapped Spearman correlations between RWI and monthly climate data indicate that baseline shrub growth at Location 2 (Adventdalen, Polygonal Tundra) is significantly positively associated with air temperature for the months May, June and July, and negatively correlated with precipitation in the preceding late autumn (November) (Fig. 2a). Shrub growth at Location 5 (Ny-Alesund, Westbyelva) shows significant positive correlation with air temperatures in June and July, and a positive correlation with precipitation in the preceding early winter (December) (Fig. 2b). Monthly averaged temperatures for the two locations in November and December were below zero (NCCS, 2025), suggesting that the significant associations with precipitation relate to snowfall. Seasonally aggregated bootstrapped Spearman correlation analysis suggests that for both sites, only summer season temperature (JJA) is significantly correlated to tree-ring growth of *S. polaris*. Seasonal climate-growth correlations indicate no association with previous summer season temperature or precipitation, and a rather similar overall pattern of seasonal climate - growth associations for the two sites (Fig. S4). Seasonal snow depth and rain-on-snow variables (Fig. S7) showed little correlation with tree ring growth, both in a partial correlation analysis correcting for the influence of summer temperature (Fig. S5) and direct Spearman correlation values (*data not shown*). Partial Spearman correlation values showed a significantly negative association between RWI and spring (MAM) season rain-on-snow totals for Location 5 (Ny-Alesund, Westbyelva) (Fig. S5b), and a tendency for positive association between winter (DJF) snow depth and RWI for Location 2 (Adventdalen, Polygonal Tundra) (Fig. S5a).

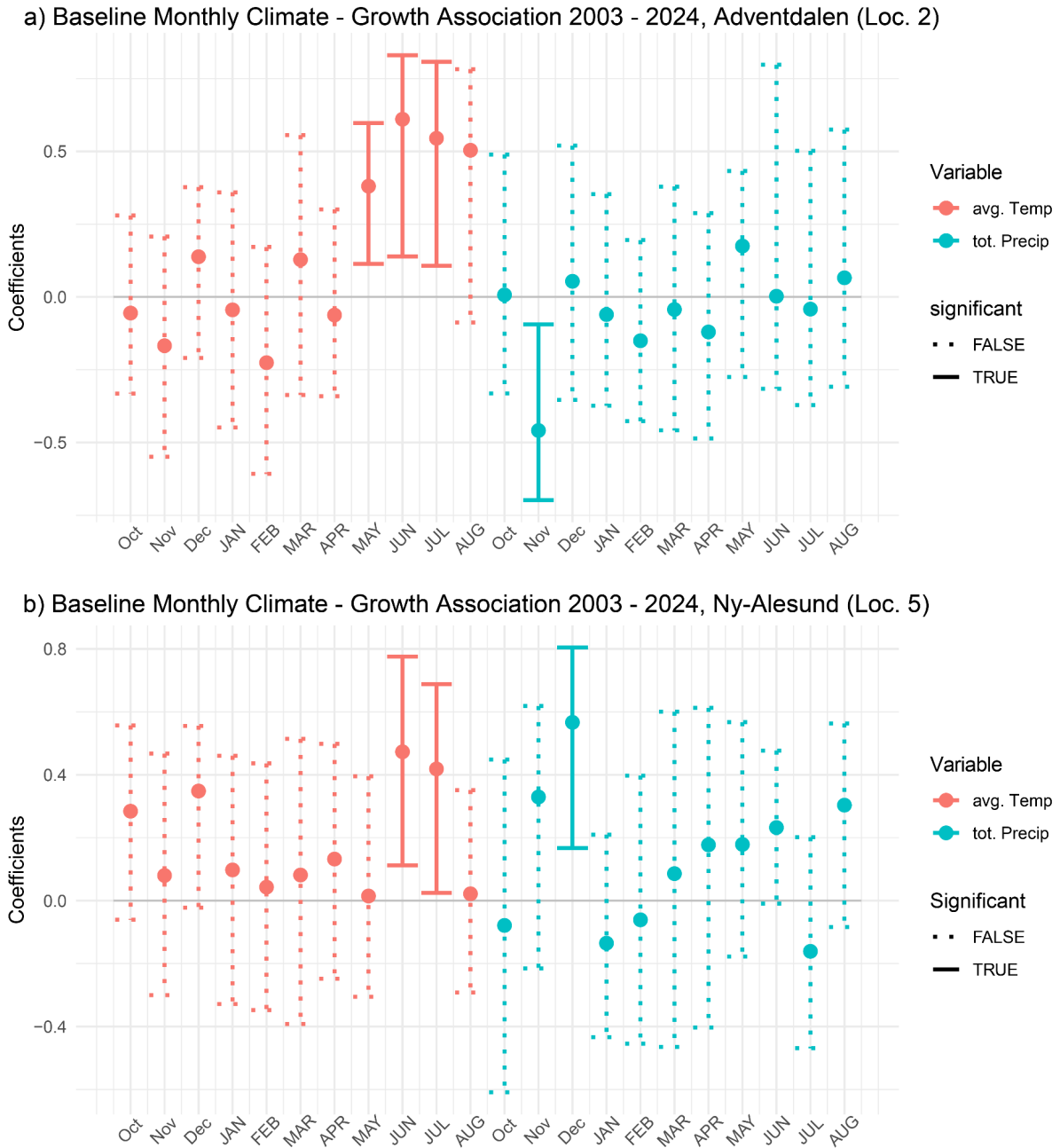


**Figure 2)** Monthly climate-growth associations for air temperature and precipitation for **a)** Location 2 (Adventdalen, polygonal Tundra) and **b)** Location 5 (Ny-Alesund, Westbyelva). Dots and vertical lines indicate the average Spearman correlation coefficient and the 95% confidence interval (CI), respectively. Solid lines indicate a significant correlation based on whether the 9% CI included zero or not. For months on the x axis, capital letters indicate months within the same calendar year, and small letters indicate months in the preceding calendar year.

## Impact of Experimental Rainfall Treatments

Linear mixed-effects models indicated no significant ( $p > 0.05$ ) Treatment:Year interaction on shrub-level RWI (accounting for shrub-level random intercepts) for Location 2 (Adventdalen, Polygonal Tundra), with only “Year” as a significant fixed effect (Table S7). This indicates that the experimental rainfall treatment did not significantly impact shrub radial growth (Fig. 3a), after accounting for age-related growth dynamics and shrub-level variability, and no post-hoc test was performed. A similar model for Location 5 (Ny-Alesund, Westbyelva) indicated a significant ( $p < 0.01$ ) Year:Treatment interaction, as well as a significant ( $p < 0.001$ ) “Year” factor (Table S8), indicating that the experimental rainfall treatment affected shrub growth differentially in different years (Fig. 3b). Post-hoc tests of pairwise treatment differences per individual year (Table S9) revealed significantly higher RWI shrub-level RWI values in E (early summer irrigation 2023) plots in 2024 compared to C (control) and I (late summer irrigation 2022) plots (Fig. 3b). A tendency ( $p = 0.051$ ) was observed for higher RWI in L plots compared to C plots in 2024. Additionally, L plots (late summer irrigation 2023) showed higher RWI values than E plots in 2022. Since the E and L treatments were not carried out until 2023, this indicates a pre-existing contrast unrelated to our treatment. No other significant differences among treatments were identified prior to the experimental rainfall treatments (but see tendency for  $C > I$  in 2019, Fig. 3b). Lack of significant contrasts between C and I plots in 2022, and C, E and L plots in 2023, indicates that the experimental rainfall treatment did not induce same-year effects in shrub radial growth.

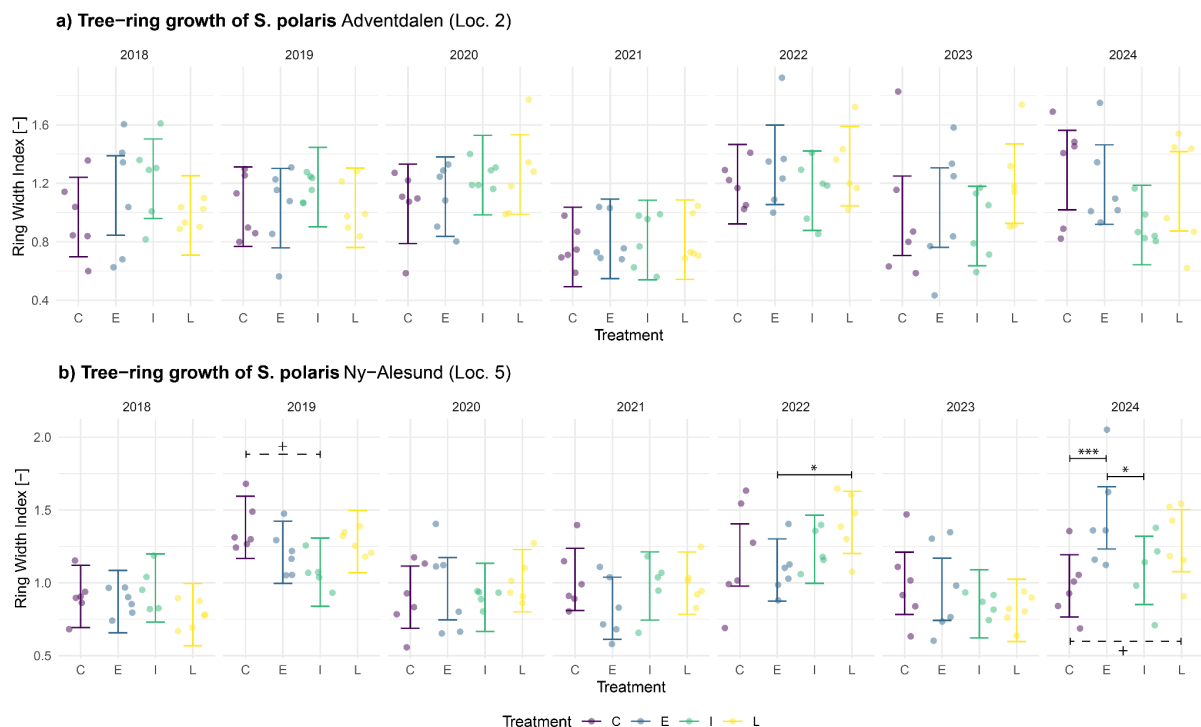


**Figure 3)** Ring-Width Index (RWI) per treatment over the common period 2018-2024 for **a)** Location 2 (Adventdalen, Polygonal Tundra) and **b)** 5 (Ny-Alesund, Westbyelva). Jittered dots indicate shrub-averaged RWI, vertical lines indicate the estimated 95% confidence interval (CI) per treatment per year. Horizontal black lines indicate significant pairwise contrasts (solid) or tendencies (dashed) based on post-hoc tests, with +  $p < 0.1$ , \*  $p < 0.05$ , \*\*  $p < 0.01$ , \*\*\*  $p < 0.001$ .

We repeated the same analysis on section-level RWI values for root collar, root and shoot sections, additionally testing for a three-way interaction between Year, Treatment and Section. RWI values for shoot ends were omitted, as these were not measured for each shrub in cases where they had an insufficient number of rings. For both sites, we found no indication of significant interactions with Section ( $p > 0.05$ ), indicating that Treatment effects did not differ among root, root collar and shoot tissues (Table S10 - S11 & Fig. S8).

## Discussion

We experimentally tested the impact of heavy rainfall events in summer on the radial growth of *Salix polaris* on Svalbard during a succession of anomalously warm summers (Fig. S6a). Baseline climate-growth associations of the two successfully sampled and cross-dated sites indicate little correlation with precipitation compared to that of summer temperature (Fig. 2). We found no same-year effects of heavy summer at either site (Fig. 3), but a positive legacy effect of rainfall addition was observed in one of the sites (Fig. 3), indicating that effects of heavy rainfall may be delayed and spatially dependent. We found no strong differences in root, root collar or shoot response to rainfall treatments, which suggests that within-shrub resource allocation patterns were not strongly affected (Fig. S8). We significantly extend upon the existing tree-ring knowledge base for Svalbard (Table 3), and identified baseline climate-growth associations that are in line with existing evidence for Svalbard (Fig. 2, Table 3). The low proportion and relatively young age of successfully cross-dated shrub ring-width series (Table 2, S3) testifies to the difficulty of the sample material, further supported by the relatively low average ring width increment (Table 2) compared to that reported earlier studies on the same species (Le Moullec et al., 2020, Opała-Owczarek et al., 2018, Owczarek and Opała-Owczarek, 2016, Buchwal et al., 2013). The implications of these and other potential limitations of our study are discussed further. We end with an outlook on growth of *S. polaris* on Svalbard under expected future rainfall and temperature dynamics.

### Legacy Effects in Rainfall Response; an Overlooked Aspect in Climate-Growth Studies?

Using a rainfall manipulation treatment, and analysis of age-detrended shrub ring widths across treatments, we found that adding rainfall did in most cases not significantly enhance shrub radial growth. Baseline-climate growth analysis also showed no overall significant influence of same-summer (Fig. 2) or previous summer's rainfall (Fig. S4) for either site. However, a lagged effect of experimental wetting was evident in one out of two analysed sites, where shrubs that had received irrigation in early summer in the previous year (2023) outperformed control shrubs that had not received rainfall (Fig. 3). Weather conditions for past decades show record-breaking temperatures for the period 2022-2024 (Fig. S6a) (van den Broek et al., 2025). Furthermore, the site at which the significant legacy effect was found (5 - Ny-Alesund, Westbyelva), had drier topsoil throughout the years of treatment whereas the other site showed consistently high soil moisture levels (Magnússon et al., 2024). This is not entirely reflected in precipitation data, which show moderate rainfall levels for 2022-2024 for both sites (Fig. S6b). This likely reflects the role of evapotranspiration and local controls on soil moisture levels in addition to rainfall totals per se. Furthermore, a study on senescence of *S. polaris* in Adventdalen found that enhanced soil moisture can extend the growing season of *S. polaris*, whereas complete saturation had adverse effects (Andersen et al., 2025). Hence, we infer that the degree to which (multi-year) drought limitation is lifted, rather than rainfall level per se, shapes the growth of *S. polaris* on Svalbard, and that occurrence of such drought limitation is highly site specific.

The effect of later summer irrigation in the same site in 2023 had a less clear legacy effect ( $p < 0.1$ , pairwise comparison of LS vs. C) compared to earlier summer irrigation ( $p < 0.001$ , ES vs. C). Similarly, no lagged effects were evident as a result of the late summer 2022 rainfall addition (Fig. 3). This could suggest that there is a critical time window beyond which the

alleviation of summer drought (2022 was a warm and dry summer) does not benefit shrub growth anymore. Alternatively, the overall poorer growth in 2023 across sites and treatment (Fig. 3) could suggest that potential legacy effects of the 2022 treatment were overshadowed by other growth limitations (e.g. relatively late snowmelt, Fig. S7a). This may have similarly masked any significant impact on shrub growth of the 2023 treatments in the same year.

Our findings are in line with evidence from North-Eastern Siberia, reporting spatially and temporally divergent climate-rainfall associations and delayed effects of previous summer's rainfall on radial growth of *Betula nana* (Magnússon et al., 2023). It further underscores findings from Greenland and Alaska, reporting reduced growth of *Betula nana* under prolonged dry and warm conditions (Gamm et al., 2018), and reduced temperature sensitivity of *S. pulchra* in drier habitats (Ackerman et al., 2017). This demonstrates the complex role of rainfall and moisture availability in co-regulating shrub growth, and highlights how such drivers are not readily evident from baseline climate-growth correlations without experimentation or explicit consideration of multi-year moisture dynamics, legacy effects and spatial gradients.

We originally hypothesized that *S. polaris* individuals would display differential above- and belowground resource allocation under heavy rainfall extremes. However, we did not find indications that the response of wood increments differed among root, root collar and shoot in response to our rainfall treatment (Fig. S8, Table S11-S12). Previous work on Svalbard also found that ratios of above- and belowground wood growth were only significantly related to temperature, and not to precipitation, with higher investment in belowground growth in warm summers (JJA) and higher aboveground growth after warm springs (MAM) (Buchwal et al., 2013). This suggests that within-shrub allocation of wood growth is driven more by temperature or growing season onset than by rainfall, even under consecutively warm and dry summers.

Finally, an earlier study of *S. polaris* climate-growth associations on Svalbard study found a negative rather than positive association of shrub radial growth and summer precipitation, which was attributed to reduced solar radiation (Buchwal et al., 2013). This highlights the fact that we only manipulated rainfall, and not solar radiation or atmospheric moisture. A fully factorial manipulation of rainfall inputs and solar radiation could provide important complementary insights.

#### Climate Sensitivity of *S. polaris* growth on Svalbard

Our baseline climate-growth analysis revealed a pattern of consistent positive association between tree-ring growth and summer temperatures, with locally variable associations with precipitation (Fig. 2, S3). No significant relations with snow depth or rain-on-snow (ROS) totals were observed (Fig. S7). However, these data are available for a shorter timespan (2009 onwards), and ROS totals were calculated according to Vickers et al. (2022) based on daily temperature and snow depth data. This may not fully capture actual ROS events, or spatially heterogeneous dynamics of basal ice formation (Peeters et al., 2019). Similarly, Le Moullec et al. (2020) found relations between tree-ring growth and ROS to be spatially variable. Table 3 synthesises monthly and seasonal climate-growth associations reported for Svalbard in earlier literature, alongside our own findings. We do not find strong

discrepancies of our findings with the existing body of research, despite our relatively short timeperiod and challenging sample material, providing confidence in our cross-dating.

While the positive association of shrub radial growth with summer air temperature is rather consistent among studies, the high variability in observed precipitation and ROS effects suggests that precipitation effects may indeed be highly context dependent (Le Moullec et al., 2020, Magnússon et al., 2023). Based on observed strength of correlation and effects sizes in this study and those in Table 3, we expect summer temperatures to remain the most influential driver of wood growth in *S. polaris*, with context-dependent secondary effects of rainfall and winter conditions. It is important however to note the higher degree of uncertainty and difficulty in accurately capturing local hydroclimatic factors such as winter thaw and refreeze, ROS and moisture availability from snowmelt over multidecadal periods (Peeters et al., 2019, Owczarek and Opała-Owczarek, 2016). This may have additionally contributed to their less uniform role.

While not part of our research questions, we observe that the period of summer temperature sensitivity appears to differ among sites and studies (note that in Table 3, Le Moullec et al. (2020) did not evaluate different month ranges per site). Our sites show a comparatively early season temperature sensitivity, except for the Ny-Alesund site. Similarly, the longest available and southernmost record (Bjørnøya) (Owczarek et al., 2020) shows relatively early and extended temperature sensitivity. This could suggest a pattern of sensitivity towards earlier months' temperatures under earlier snowmelt and onset of the growing season, with the amount of monthly correlations that are highlighted as significant likely also depending on the different length of available records. A similar limitation could explain why we did not find a significantly negative effect of ROS (but see negative partial correlation with spring ROS, Fig S7b), while Le Moullec et al. (2020) did.

Table 3) Overview of current literature on climate-growth associations in *S. polaris* for the Svalbard archipelago

Study	Location	Period	Temp. <sup>1</sup>	Prec. <sup>1</sup>	ROS <sup>1</sup>	Other <sup>2</sup>
Buchwal et al. (2013)	Petuniabukta	1963-2011	+ (6-8)	+ (-11) - (6-8)	n.c.	n.c.
Le Moullec et al. (2020)	Ny-Alesund	1986-2014	+ (7)	n.s.	- (-11:4)	Spring onset date: n.s.
Le Moullec et al. (2020)	Sørkapp	1989-2014	+ (7)	n.s.	n.s.	Spring onset date: n.s.
Le Moullec et al. (2020)	Edgeøya	1976-2014	+ (7)	n.s.	n.s.	Spring onset date: n.s.
Le Moullec et al. (2020)	Barentsøya	1974-2014	+ (7)	n.s.	n.s.	Spring onset date: n.s.
Le Moullec et al. (2020)	Kapp Linné	1977-2014	+ (7)	n.s.	- (-11:4)	Spring onset date: n.s.
Le Moullec et al. (2020)	Hornsund	1962-2014	+ (7)	n.s.	n.s.	Spring onset date: n.s.
Le Moullec et al.	Semmeldalen	1985-2014	+ (7)	n.s.	n.s.	Spring onset

(2019)						date: n.s.
Opala-Owczarek et al. (2018)	Fuglebekken	1946–2011	n.s.	+ (6-8)	n.c.	Snowmelt date: n.s. PDD <sup>4</sup> : n.s.
Owczarek et al. (2020)	Bjørnøya	1922–2016	+ (3,5-9)	+ (-5,2,4,8) - (-6)	n.c.	n.c.
this study	Ny-Alesund	2003 - 2024	+ (6-7)	+ (-12)	n.s. <sup>3</sup>	Snow depth: n.s. <sup>3</sup>
this study	Adventdalen	2003 - 2024	+ (5-7)	- (-11)	n.s. <sup>3</sup>	Snow depth: n.s. <sup>3</sup>
this study	Endalen	2001 - 2023	+ (5,7) - (F)	n.s.	n.c.	n.c.

- 1) Only significant effects are listed, with + or - indicating the direction of the effect, and the numbers in brackets indicating the corresponding months. "-" indicates the previous year. Multiple significant relations can exist for different months. n.s. indicates that the variable was not significant in any period ( $p > 0.05$ ). n.c. indicates that this variable was not considered.
- 2) Name of the other climatic variable considered, then same as <sup>1</sup>
- 3) Based on a shorter time period (2010 - 2024).
- 4) Positive degree days

## Recommendations and Limitations

Earlier dendrochronological studies for Svalbard (Buchwal et al., 2013, Le Moullec et al., 2019, Le Moullec et al., 2020, Opala-Owczarek et al., 2018, Owczarek and Opala-Owczarek, 2016, Owczarek et al., 2020) have often used a more extensive hierarchical cross-dating process with well over 4 segments per shrub. Since we aimed to evaluate the impact of a plot-level treatment, and due to the time-consuming nature of tree-ring analysis, we prioritized replication of experimental units rather than within-shrub replication. Using a higher amount of segments per shrub could have resulted in more certainty during the cross-dating process. Even with a back-up sample per plot, and cutting of new sections for poorly discernible samples, we were unable to accurately measure or cross-date a shrub series for every single plot. Only two out of four sampled sites showed a high enough proportion of measurable samples and high enough interseries correlation of half chronology samples. We further observed relatively small tree-ring increments compared to earlier studies (Buchwal et al., 2013, Le Moullec et al., 2019, Opala-Owczarek et al., 2018), as well as differences in tree-ring size (Table 2 & S4) and discernibility among different sampling sites. Samples from Endalen and Ny-Alesund (Location 5) showed larger and more clearly distinguished tree-rings and shoot - root collar - root morphology compared to samples from the polygonal tundra meadow in Adventdalen (Location 2), which matches earlier observations that *S. polaris* individuals in moist habitats with dense vegetation form more complex belowground structures (Le Moullec et al., 2019). Furthermore, the two locations that had to be omitted altogether featured a history of rather intensive human land use (Adventdalen Loess terrace, many damaged sections) and high within-site variability in soil and hydrological conditions (Location 4, Endalen slope, low visual fit among initial samples). This indicates that particularly for environmentally heterogeneous sites (Location 4), moist and densely vegetated sites (Location 2) and heavily disturbed sites (Location 1), higher replication levels are necessary.

Even though disruptive and time-consuming, future studies should ideally also sample more individuals from a single experimental unit (plot), so that there is a better chance of obtaining a measurable sample within a comparable age range. The fact that no significant difference in shrub age was found among treatment classes means that it is unlikely that identified treatment effects in this study were confounded by shrub age, although with a small sample size, such confounding effects may easily occur. With a larger set of samples per experimental unit, researchers could also stratify measured shrubs over age classes and include interactions of treatment effect with shrub age or other shrub-level traits. Since site conditions at the two locations where we could perform successful crossdating were rather environmentally homogeneous (Magnússon et al., 2024), we expect little confounding effects of plot-level variability in the present analysis.

Our samples and chronologies contained relatively young shrubs (Table 2) compared to many earlier studies (Buchwal et al., 2013, Le Moullec et al., 2019, Le Moullec et al., 2020, Opała-Owczarek et al., 2018, Owczarek and Opała-Owczarek, 2016, Owczarek et al., 2020). This implies that our identified baseline climate-growth relations and the impacts of rainfall treatments may pertain specifically to younger shrub individuals, and further research would be necessary to assess whether similar mechanisms apply to older shrub individuals. The young age of our samples may be a result of our plot-based sampling strategy, which was unbiased towards age and size in order to obtain locally representative data, while traditional dendrochronological studies tend to favour large individuals (Myers-Smith et al., 2015b). This further suggests that our findings may be more representative of the actual age and size composition of Svalbard shrub populations. Potential limitations, however, are less certainty during crossdating, shorter time periods and statistical power for chronologies and climate-growth analysis, and a lower age range to inform our detrending procedure, which may have led to less robust chronologies and climate-growth associations (see for instance relatively low mean sensitivity and interseries correlations in Table 2). The fact that our identified climate-growth associations closely match those of earlier studies (Table 3) implies that no gross inaccuracies during cross-dating have occurred.

Finally, radial growth proxies come with inherent limitations. While demonstrated to correlate with shrub or vascular plant community biomass (Le Moullec et al., 2019), they do not capture potential effects on recruitment and mortality dynamics, which have been found to also be sensitive to rainfall extremes and moisture availability (Li et al., 2016, Magnússon et al., 2023). They may also not capture instantaneous above-ground responses in for instance shoot length, leaf traits and timing of senescence (Keuper et al., 2012, Andersen et al., 2025). This also prevents us from making any inferences about their role in effectuating legacy effects. An earlier study attributed observed legacy effects of rainfall to changes in above-ground carbon assimilation and assimilate storage and bud development (Blok et al., 2011), and monitoring a more holistic range of above- and belowground variables could provide important insights into the mechanisms behind legacy effects.

### Implications for Shrub Growth on Svalbard

Similar to earlier studies, we found summer temperatures to be the main climate driver of shrub growth of *Salix polaris* on Svalbard. While earlier studies have predominantly found

correlations with June-July-August temperatures, we found evidence of May temperatures already influencing shrub growth in locations with earlier snowmelt and warmer summers (Fig. 2 & S3). This could signal a shift towards sensitivity to temperatures in earlier months with earlier snowmelt conditions and earlier start of the growing season on Svalbard. It is important to acknowledge that our experiment was carried out over the course of three consecutive summers with record-breaking temperatures with comparatively low rainfall particularly for Ny-Alesund (2022 - 2024, Fig. S6). Baseline climate - growth relations did not show significant rainfall - growth association. However, experimental results show that rainfall impacts may be site-specific and delayed, and were particularly evident in the drier Ny-Alesund site. This suggests that baseline climate - growth associations constructed for past decades without consideration for spatial heterogeneity and legacy effects may not fully capture the role of newly emerging climate extremes in a rapidly warming Svalbard. With expected trends of continued warming and increasing year-to-year variability in rainfall dynamics on Svalbard (Hanssen-Bauer et al., 2019), rainfall dynamics may be expected to shape the growth of keystone shrub species *S. polaris* in spatiotemporally complex ways. Although based on evidence from only two sites, patterns identified in our study suggest that shrubs growing in exposed landscape positions in relatively dry soils show reduced growth particularly after consecutive summers with warm and dry conditions, and that apart from lifting such drought limitations, heavy rainfall events do not influence radial growth.

## Supplementary Information

### Text S1 - Tree-Ring Sample Processing & Measurement Workflow

#### *Micro-thin Sectioning*

We cut 15-20  $\mu\text{m}$  thin sections perpendicular to the axis of elongation of each 2cm shrub segment using a GSL1 sledge microtome (WSL, Birmensdorf, Switzerland). We followed best practices of Gärtner and Schweingruber (2013). Each section was visually inspected under a microscope for damage, side-branches and misalignment against wood vessel orientation, and sectioning was repeated if necessary. For very small samples (most notably the aboveground shoot ends), the segment was placed between two halves of a wine cork to facilitate micro-thin cutting without compressing and damaging the stem too much. Samples were then stained using a safranin/astra blue mixture for 15 minutes to enhance visual contrasts between various wood tissues, and rinsed using demi water and ethanol solutions of increasing purity (50, 70, 96 and 100%). Finally, samples were washed with Roti®-Clear liquid and embedded on glass slides in Roti®-Mount resin.

#### *Sample Imaging*

Samples were photographed and digitized using a Leica DM 2500 microscope with Flexacam C3 camera (both Leica Microsystems, Wetzlar, Germany). Images with camera-calibrated scale bar and dpi settings were exported at 4000 by 3000 pixel resolution using LAS X version 4.13 (Leica Microsystems, Wetzlar, Germany). If needed, overlapping images were taken at higher magnification and stitched together using PTGui v. 2.9.1 (New House Internet Services, Rotterdam, The Netherlands).

#### *Tree-Ring Measurement & Cross-dating*

We applied a serial sectioning and hierarchical crossdating approach to measure tree-ring widths (Hallinger et al., 2010, Myers-Smith et al., 2015b, Wilmking et al., 2012), using three radii and four sections per shrub. Tree-ring widths were measured along radii per section image in Coorecorder version 9.0 (Cybis, Saltsjöbaden, Sweden). In case a shrub showed signs of damage, a side branch or very unclear rings on a particular area of the cross-section, two radii were deemed acceptable if no better cross-section could be obtained. We measured radii for all four segments of a shrub. We measured tree rings without a reference initially, usually starting with the root collar sample since these samples often displayed the most clearly visible rings and most rings of all segments of the same shrub. We then visually compared measurement series to a site reference series (see *Reference Chronologies and Half-Chronologies*) and inspected the image and series for missing rings. We then compared and cross-dated radii within a segment, and then segments within a shrub. Radii per segment were averaged in CDendro version 9.0 (Cybis, Saltsjöbaden, Sweden). In many cases, however, the above-ground shoot-end was not considered further due to an insufficient number (5 or less) of rings. In case a shrub showed extensive damage, poorly discernible rings or poor visual fit to the site reference series, we discarded the measurements and cut either new sections from the same 2cm shrub fragments, or cut the second sample for the same plot.

#### *Reference Series*

During cross-dating, we used reference chronologies and half-chronologies to aid in cross-dating. For Ny-Alesund, we used a site chronology from Le Moullec et al. (2020) for 1986-

2015 as a reference. For Adventdalen and Endalen, we used a reference series of seven shrubs collected in 2023 (see Text S2). For each site at which tree-ring samples were collected, we first independently measured tree-ring series for eight to ten root collar (and in a few cases root or shoot) images of different shrubs that showed clear and discernible rings, and then compared series among each other (Table S3) and to the appropriate reference series. If these showed sufficient visual match, we developed a half-chronology by averaging the mean-detrended samples and reference chronology. In case of mismatches among sample radii and sections, the half-chronologies were used as a reference to detect missing rings. We adopted a fairly restrictive approach to adding missing rings, only adding rings in case the section image showed clear signs of missing rings (small areas where wedging tree ring boundaries that were overlooked, obviously thickened tree ring boundaries), or sufficient tree ring measurements before and after the suspected missing ring were available to confirm significant increases in inter-series (within the same shrub and towards the site average) correlation.

### *Series Inspection*

Individual section-averaged tree-ring series were combined per experimental location (Table 1) and exported as Tucson format (.rwl) decadal files. A final round of visual checks for within-shrub and among-shrub fits was performed in WinTSAP v. 4.70d (Rinntech, 2017) by manually comparing and shifting individual series against a location average and other sections within the same shrub individual. In case the fit of an individual section improved drastically by shifting the series by one year, the original Coorecorder coordinate files and images were inspected for completely missing rings at the section- or shrub level again.

### *Series Detrending*

.rwl datasets were loaded into R version 4.4.1 and detrended and inspected using the dplR package (Bunn, 2008). To correct for age-related growth trends at the section level, we fit an age-dependent cubic smoothing spline with an initial stiffness of 20 years, growing progressively stiffer for each incremental tree ring spline. We constrained the detrending series to a slope of zero at the end of the series in order to account primarily for juvenile growth deviations. This procedure is described in more detail in Cook and Kairiukstis (1990) and Melvin (2004). Raw series were detrending by division against fitted values and interseries correlation was computed according to Briffa and Jones (1990). We corrected for temporal autocorrelation (“pre-whitening”) using a first-order autoregression function. Out of various detrending algorithms that we explored (spline, mean, c-method and regional curve standardization), we chose an age-dependent spline and initial stiffness value based on interseries correlation values and spaghetti plots of detrended and undetrended series, ensuring that our choice for detrending method accurately removed juvenile growth patterns and maximized synchronicity of year-to-year growth variation among sections.

We then exported age-detrended and pre-whitened residual RWI values at the section-level, shrub-level (averages of all segments within a shrub) and site-level (site chronology, average of all shrubs within a site). For the site chronologies, we used a residual chronology with a minimum sample depth of three individuals. We also removed the RWI values of all treated plots (I plots from 2022 onwards, E and L plots from 2023 onwards) to obtain site-level chronologies of shrub radial growth under baseline conditions. We did not make separate root, root collar and shoot chronologies due to limited series length root and particularly shoot samples.

## Text S2 - *S. polaris* Reference Series Endalen

We conducted a feasibility study for tree-ring measurement of *S. polaris* in summer 2023, sampling 13 shrubs at a river terrace at the entrance of Endalen (Fig. S1) close to experimental sites 1 - 4 (Table 1). Shrubs were excavated and processed as described in Text S1, using a more extensive serial sectioning approach (one to two root segments, one root collar, one to two belowground branch samples and one aboveground branch sample, see Fig. S1c). Hierarchical crossdating and chronology development was performed as described in Text S1, with a Svalbard-wide *S. polaris* chronology from Le Moulec et al. (2020) as a reference for 1962 - 2014. For this reference series, we only included samples that could be measured and cross-dated visually, and shrub means were constructed from a variable number of sections. seven out of 13 shrubs showed significant ( $p < 0.05$ ) correlation towards the rest of the dataset and were retained for chronology development.



**Figure S1) Sampling location (a,b) and strategy (c) for a pilot study and development of a reference chronology for cross-dating of sample material from Adventdalen & Endalen. c shows a typical morphology for *S. polaris* samples growing in isolated patches in well-drained sites, with a root collar, central tap root and laterally branched (predominantly belowground) shoot system. Blue tape markers indicate where segments were sampled.**

Figure S2 and S3 show the chronology and climate-growth associations for the chronology developed from the 7 selected shrub samples from this pilot study, derived according to the methods described in Text S1 and the main text ("*Baseline Climate Growth Association*"). Table S4 shows statistical properties of the tree-ring dataset of shrub averages.

## Irrigation Water Characteristics

Table S1) Concentration of key nutrients and elements in irrigation water and rainwater samples. Measured through Atomic Absorption Spectroscopy against calibration series. All 50mL samples were passed through a 0.45 µm filter, stored in clean HDPE bottles and acidified with citric acid. All concentrations in mg/L.

<b>Location</b>	<b>N-NO3</b>	<b>N-NH4</b>	<b>P-PO4</b>	<b>S-SO4</b>	<b>Na</b>	<b>Ca</b>	<b>Mg</b>	<b>K</b>	<b>Cl</b>
1- Loess Terrace (July 2022)	0.01	0.03	0	198.6	77.0	87.4	35.4	9.73	128.2
2- Polygon Tundra (July 2022)	0.18	0.04	0	67.0	20.4	18.1	8.7	4.7	4.6
3- Endalen Terrace (July 2022)*	0.08	0.02	0	64.5	5.4	8.3	3.5	1.11	3.5
4- Endalen Slope (July 2022)*	0.08	0.02	0	64.5	5.4	8.3	3.5	1.11	3.5
5- Ny-Ålesund (July 2022)	0.07	0.12	0	199.9	17.3	54.3	23.4	5.8	3.0
1- Loess Terrace (June 2023)	0.03	0.12	0.1	64	58.3	46.2	22.4	4.9	136.7
2- Polygon Tundra (June 2023)	0	0.08	0.08	24.4	15.1	10.7	5.5	2.7	22.9
4- Endalen Slope (June 2023)	0.1	0.12	0.09	26.2	6.7	6.3	2.7	0.6	47.9
Rain (June 2023)**	0.06	0.10	0.08	5.1	0.9	1.0	0.2	0.8	61.1
Rain (July 2023)**	0.07	0.07	0.08	5.1	0.9	1.6	0.4	0.6	71.8

\*) The stream from which irrigation water was supplied was the same for Locations 3 and 4.

\*\*\*) Rainfall samples were gathered in Longyearbyen outside the UNIS guesthouse using a funnel and HDPE vial, pre-cleaned with deionized water.

Table S2) Total nutrients added to plots under irrigation (in 50mm irrigation, based on table S1) compared to nutrient levels in 50mm rainwater (Table S1) and total summer season wet deposition observed in Ny-Ålesund (Kühnel et al., 2011).

<b>Location</b>	<b>added N-NO3 [mg]</b>	<b>added N-NH4 [mg]</b>	<b>added P-PO4 [mg]</b>
1- Old Aurora Station (July 2022)	0.5	1.5	0
2- Polygon Tundra Site (July 2022)	9	2	0
3- Endalen Terrace (July 2022)	4	1	0
4- Endalen Slope (July 2022)	4	1	0
5- Ny-Ålesund (July 2022)	3.5	6	0
1- Old Aurora Station (June 2023)	1.5	6	5
2- Polygon Tundra Site (June 2023)	0	4	4
4- Endalen Slope (June 2023)	5	6	4.5
Rain (June 2023)	3	5	4
Rain (July 2023)	3.5	3.5	4
Total Summer wet deposition (Kühnel et al, 2011)	24	7	n.d.

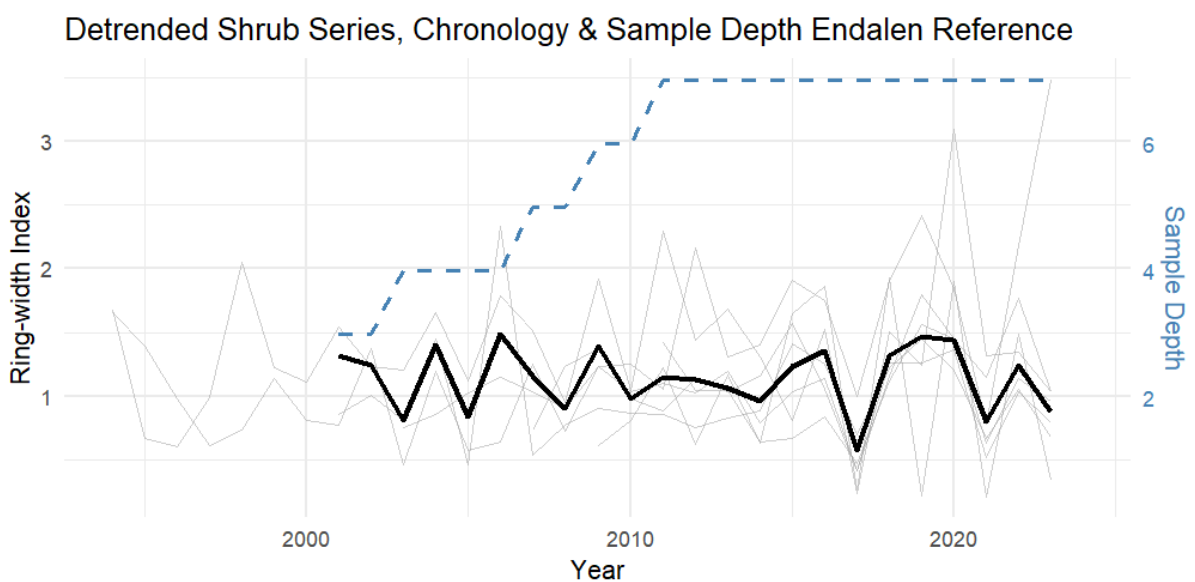
## Cross-dating Results

Table S3) Cross-dating results for the four sampled sites.

Site	Nr. Shrubs Sampled	Sufficient Undamaged Samples?	Nr. Shrubs Half Chronology "nuggets")	Half Chronology Interseries Correlation <sup>1</sup>	Cross-dating continued ?	Nr. of Shrubs successfully crossdated initially	Nr. of back-up shrubs successfully crossdated	Nr. of shrubs / plots in dataset
1 - Adventdalen Loess terrace	2 x 28 (7 repl. per treatment)	n	-	-	n	-	-	-
2 - Adventdalen Polygonal Tundra	2 x 28 (7 repl. per treatment)	y	9	0.38	y	15 of 28	9 of 13	24 (6 repl. per treatment)
4 - Endalen North-facing Slope	2 x 24 (6 repl. per treatment)	y	10	0.15	n	-	-	-
5 - Ny-Alesund Westbyelva	2 x 24 (6 repl. per treatment)	y	8	0.28	y	16 of 24	7 of 9	23 (5-6 repl. per treatment)

1) Following Cook & Briffa (1990)

## Results Endalen Chronology



**Figure S2) Reference Chronology Endalen Samples.** Dashed blue lines indicate sample depth (number of shrubs) per year. Grey lines indicate shrub-averaged (multiple sections) age-dependent spline detrended and pre-whitened (1st order autoregression model) RWI of individual shrubs. Thicker black lines indicate site chronology, with a minimum sample depth of 3.

**Table S4) Endalen reference Chronology Statistics** - at the level of Shrub Averaged Growth Series

Site	Nr. Shrubs	Time Span <sup>1</sup>	Mean Interseries Correlation <sup>2</sup>	Mean Sensitivity <sup>3</sup>	AR(1)	Mean ring width (mm)	Mean Age	St. dev. Age
Endalen	7	2001 (1966) - 2023	0.55	0.45	-0.07	N.A. <sup>4</sup>	26.43	15.99

- 1) Starting year indicates first year with sample depth of 3 or more series, while the number in brackets indicates oldest observed tree ring (see Fig. S2)
- 2) Following Cook et al. (1990)
- 3) Following Biondi and Qeadan (2008)
- 4) Due to a mistake in camera calibration, no accurate values of actual ring widths were obtained for this dataset. The mistake was corrected prior to the analysis of sample material for Locations 2 and 5.

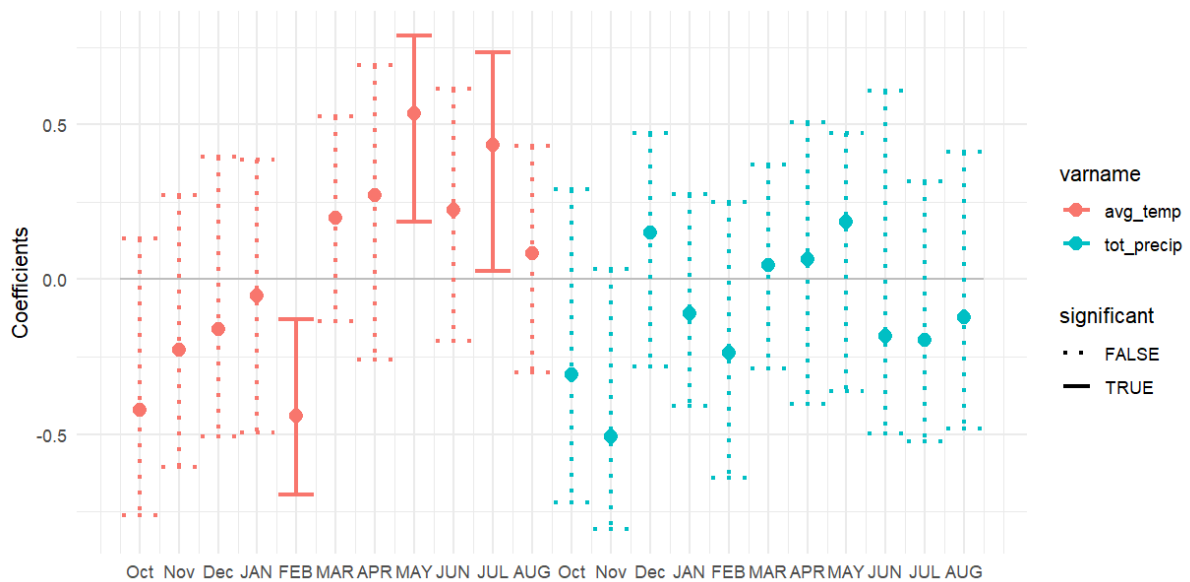


**Figure S3) Monthly climate-growth associations** for air temperature and precipitation for the Endalen Reference Chronology, 2001 - 2024. Dots and vertical lines indicate the average Spearman correlation coefficient and the 95% confidence interval (CI), respectively. Solid lines indicate a significant correlation based on whether the 9% CI included zero or not. For months on the x axis, capital letters indicate months within the same calendar year, and small letters indicate months in the preceding calendar year.

## Seasonal Climate Correlations

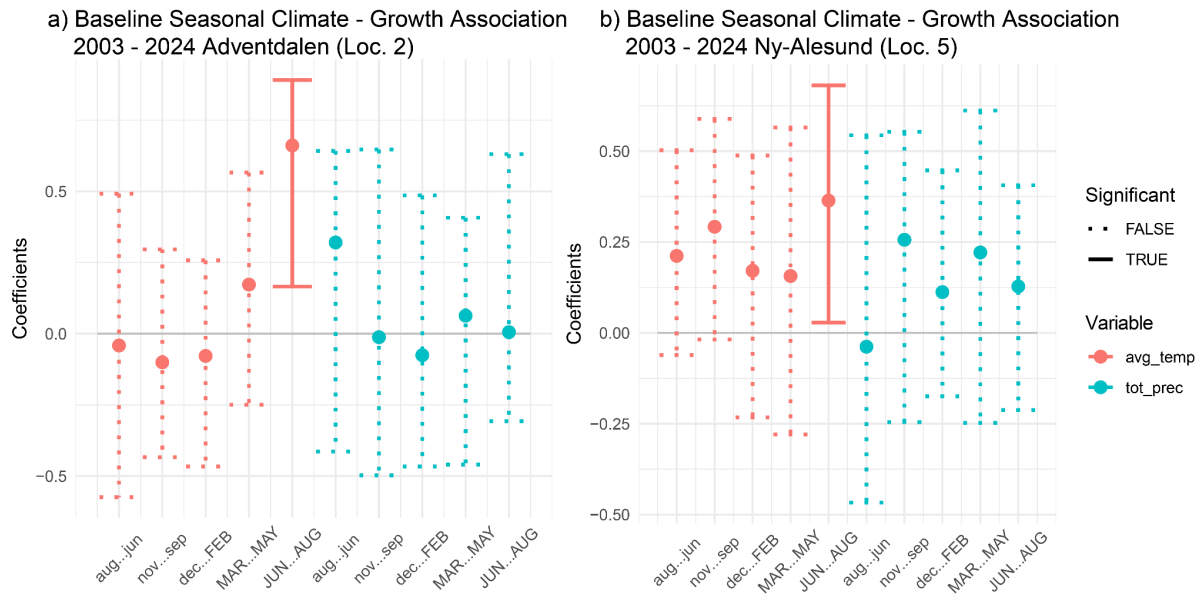


**Figure S4) Seasonal Climate - Growth Associations for a) Location 2 (Adventdalen, Polygonal Tundra) and b) Ny-Alesund (Westbyelva).** JJA, SON, DJF and MAM refer to the climatological summer, autumn, winter and spring season, respectively. Specifically, pJJA = previous year's June - August, SON = previous year's September - November, DJF = previous year's December - current year February, MAM = current year March - May, JJA = current year June-August. Dots and vertical lines indicate the average Spearman correlation coefficient and the 95% confidence interval (CI), respectively. Solid lines indicate a significant correlation based on whether the 9% CI included zero or not. For months on the x axis, capital letters indicate months within the same calendar year, and small letters indicate months in the preceding calendar year.

## ANOVA Tables of Shrub Age per Treatment Class

Table S5-S6 show type III ANOVA tables for selected models with statistics per fixed model term, using F-tests with Kenward-Roger approximation. Column names refer to sum of squares, mean squares, numerator and denominator degrees of freedom, F statistic (following Kenward-Rogers approximation) and its associated p-value. Tendencies are given as italics ( $p < 0.1$ ), significant effects in bold ( $p < 0.05$ ).

Table S5) Treatment "Effect" on age of sampled shrubs (Location 2 - Adventdalen, Polygonal Tundra)

<b>term</b>	<b>df</b>	<b>sum sq</b>	<b>mean sq</b>	<b>F value</b>	<b>p.value</b>
Treatment	3	62.792	20.931	0.567	0.643
Residuals	20	738.833	36.942		

Table S6) Treatment "Effect" on age of sampled shrubs (Location 2 - Adventdalen, Polygonal Tundra)

<b>term</b>	<b>df</b>	<b>sum sq</b>	<b>mean sq</b>	<b>F value</b>	<b>p.value</b>
Treatment	3	56.309	18.77	1.281	0.309
Residuals	19	278.3	14.647		

## Results Partial Correlation Analysis Snow Depth & Rain-on-snow

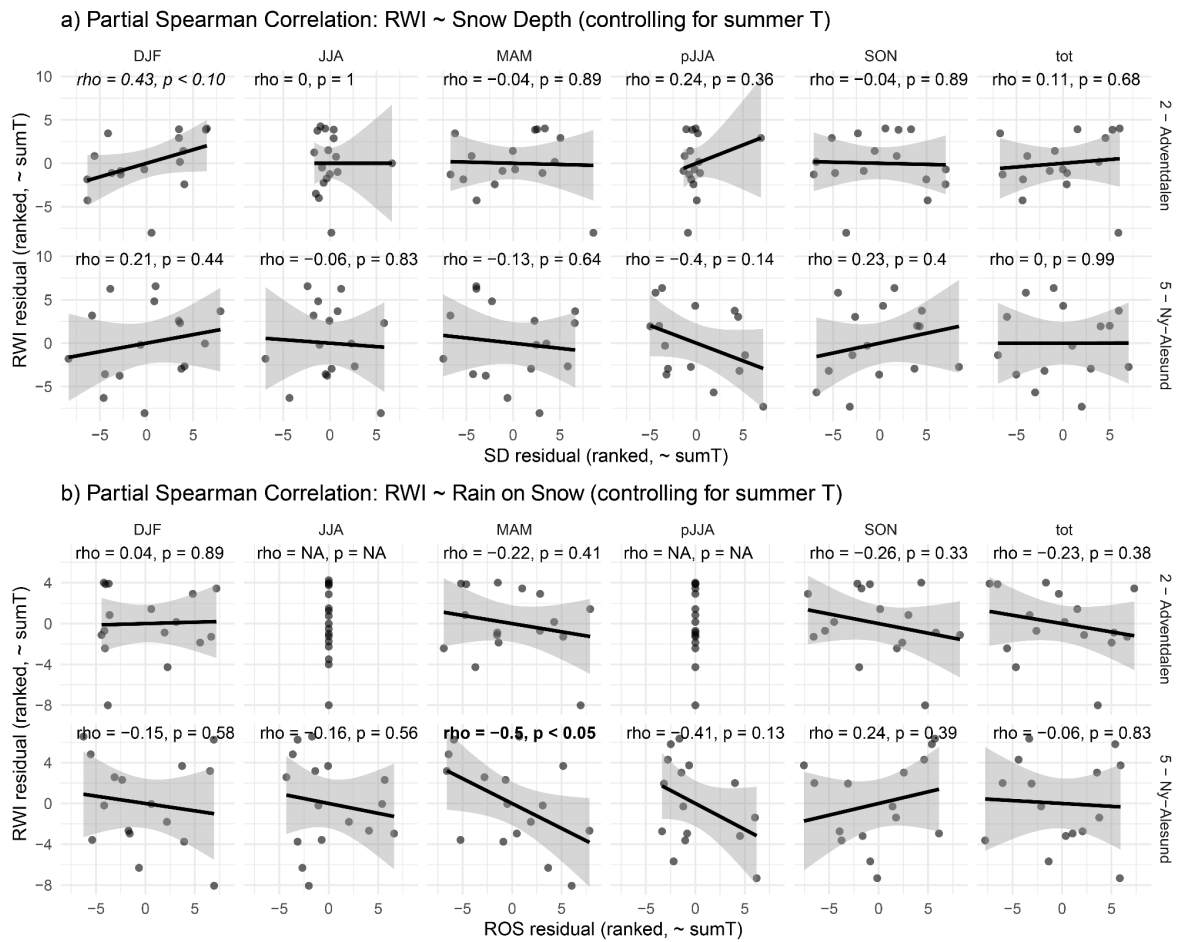


**Figure S5) Partial Spearman Correlation between a) RWI and seasonal average snow depth (SD), and b) RWI and seasonal rain-on-snow (ROS) sums. Partial Spearman Correlation values were generated based on residuals of ranked RWI, snow depth and rain-on-snow against ranked summer temperature, where summer temperature was averaged over the summer months that showed the strongest correlation with RWI in the baseline climate growth analysis (Fig. 2, May-July for Location 2 Adventdalen, June-July for Location 5 Ny-Alesund). Columns refer to separate seasons (DJF = December - February, etc), where pJJA refers to the previous summer season, and “tot” refers to the total preceding winter season (total rain on snow and averaged snow depth for SON, DJF and MAM). Lines and shaded areas represent a linear fit with a 95% confidence interval.**

## Climate Data

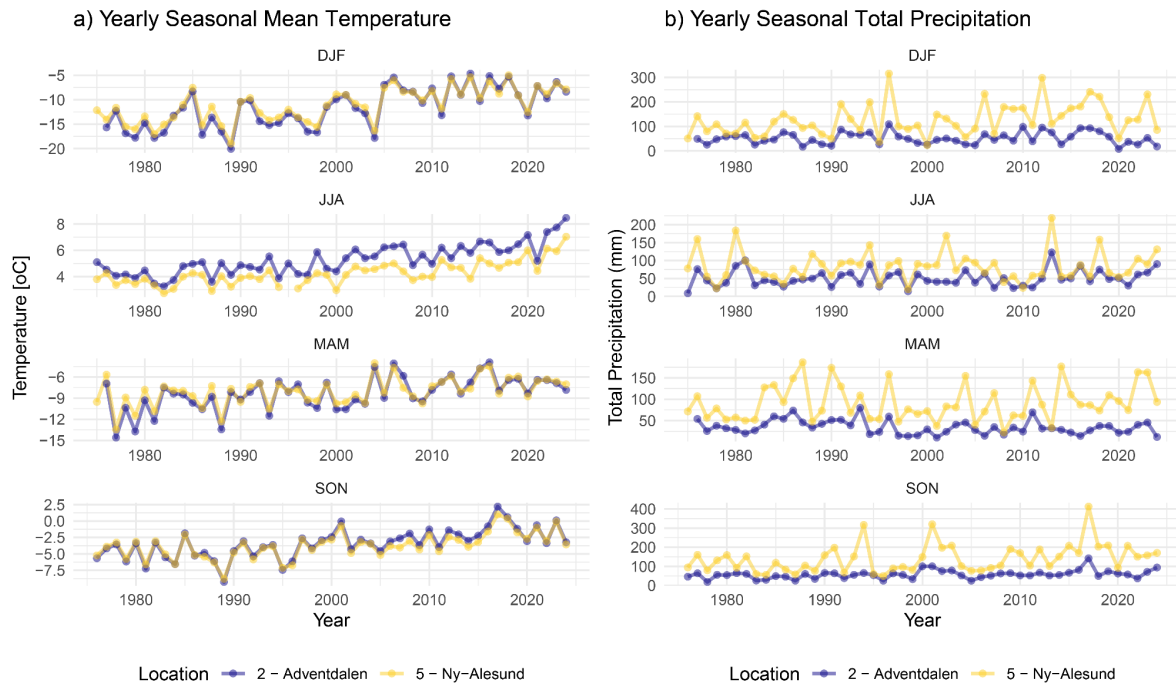


**Figure S6)** Annual dynamics of **a)** seasonal mean temperatures, and **b)** seasonal precipitation sums. Colours indicate the two different sites and weather stations (Adventdalen, corresponding weather station is Svalbard Airport SN99840 and Ny-Alesund, corresponding weather station in Ny-Alesund SN99910). DJF = December - February, MAM = March - May, etc. The months September to December refer to the year prior to that year's growing season.

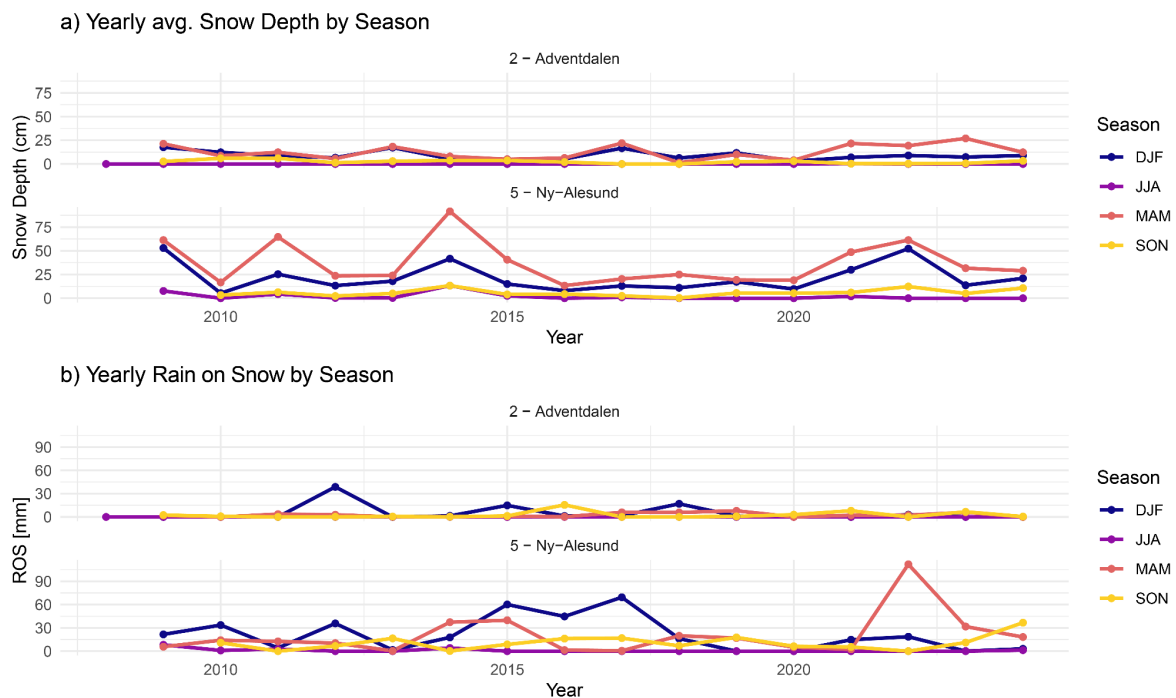


**Figure S7)** Annual seasonal dynamics of **a)** average snow depth, and **b)** rain-on-snow sums. Colours indicate separate seasons (DJF = December - February, etc). Data prior to 2008 / 2009 are not available (NCCS, 2025). The months September to December refer to the year prior to the biological growing season.

### ANOVA & Post-hoc Tables Treatment effects on RWI

Table S7-S8 and S11-S12 show type III ANOVA tables for selected models with statistics per fixed model term, using F-tests with Kenward-Roger approximation. Column names refer to sum of squares, mean squares, numerator and denominator degrees of freedom, F statistic (following Kenward-Rogers approximation) and its associated p-value. Tendencies are given as italics ( $p < 0.1$ ), significant effects in bold ( $p < 0.05$ ).

Table S9-S10 show post-hoc tests for Treatment:Year or Treatment:Year:Section interactions with  $p < 0.1$ . Post-hoc tables are given with estimated pairwise contrasts (estimate), standard errors (st. err.) and mvt-corrected p values (p. value) following Lenth (2025) among treatments at each level of "Year" and "Section".

Table S7) Shrub-level RWI - Location 2 (Adventdalen, Polygonal Tundra), 2018-2024. Type III Analysis of Variance Table with Kenward-Roger's method.

<b>term</b>	<b>sumsq</b>	<b>meansq</b>	<b>NumDF</b>	<b>DenDF</b>	<b>statistic</b>	<b>p.value</b>
Treatment	0.129	0.043	3	20	0.62	0.611
Year	3.067	0.511	6	120	7.363	1.02E <sup>-6</sup>
Treatment:Year	1.21	0.067	18	120	0.968	0.501

Table S8) Shrub-level RWI - Location 5 (Ny-Alesund, Westbyelva), 2018-2024. Type III Analysis of Variance Table with Kenward-Roger's method.

<b>term</b>	<b>sumsq</b>	<b>meansq</b>	<b>NumDF</b>	<b>DenDF</b>	<b>statistic</b>	<b>p.value</b>
Treatment	0.092	0.031	3	19	0.717	0.554
Year	3.641	0.607	6	114	14.173	5.24E <sup>-12</sup>
Treatment:Year	1.689	0.094	18	114	2.191	0.006

Table S9) Post-hoc tests for Pairwise Treatment Difference in Shrub-level RWI per Year - Location 5 (Ny-Alesund, Westbyelva).

<b>contrast</b>	<b>estimate</b>	<b>st. err.</b>	<b>Year</b>	<b>p.value</b>
-----------------	-----------------	-----------------	-------------	----------------

C - E	2.39e-02	1.19e-01	2018	0.997	
C - I	-5.51E-02	1.25e-01	2018	0.971	
C - L	1.23e-01	1.19e-01	2018	0.733	
E - I	-7.90E-02	1.25e-01	2018	0.922	
E - L	9.89e-02	1.19e-01	2018	0.841	
I - L	1.78e-01	1.25e-01	2018	0.489	
C - E	1.63e-01	1.19e-01	2019	0.526	
<i>C - I</i>	<i>3.01e-01</i>	<i>1.25e-01</i>	<i>2019</i>	<i>0.081</i>	+
C - L	9.26e-02	1.19e-01	2019	0.866	
E - I	1.39e-01	1.25e-01	2019	0.686	
E - L	-7.00E-02	1.19e-01	2019	0.936	
I - L	-2.09E-01	1.25e-01	2019	0.346	
C - E	-6.93E-02	1.19e-01	2020	0.938	
C - I	-4.82E-03	1.25e-01	2020	1	
C - L	-1.18E-01	1.19e-01	2020	0.755	
E - I	6.45e-02	1.25e-01	2020	0.955	
E - L	-4.89E-02	1.19e-01	2020	0.977	
I - L	-1.13E-01	1.25e-01	2020	0.802	
C - E	1.96e-01	1.19e-01	2021	0.361	
C - I	4.21e-02	1.25e-01	2021	0.987	
C - L	2.90e-02	1.19e-01	2021	0.995	
E - I	-1.54E-01	1.25e-01	2021	0.612	
E - L	-1.67E-01	1.19e-01	2021	0.505	
I - L	-1.31E-02	1.25e-01	2021	1	

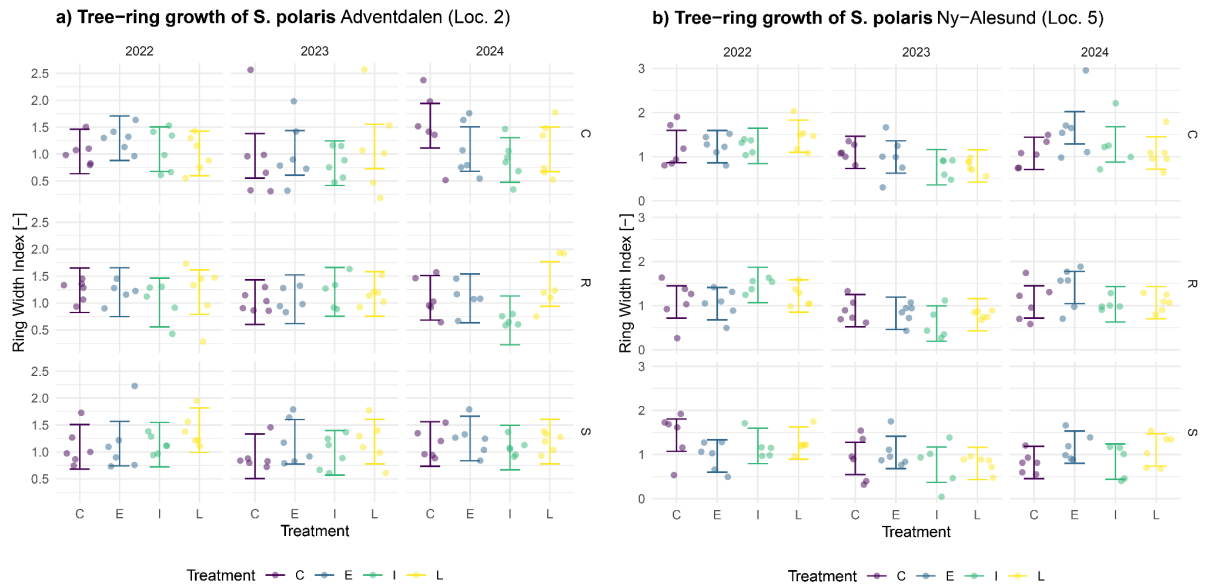
C - E	1.10e-01	1.19e-01	2022	0.792	
C - I	-4.03E-02	1.25e-01	2022	0.988	
C - L	-2.18E-01	1.19e-01	2022	0.266	
E - I	-1.51E-01	1.25e-01	2022	0.626	
<b>E - L</b>	<b>-3.29E-01</b>	<b>1.19e-01</b>	<b>2022</b>	<b>0.034</b>	*
I - L	-1.78E-01	1.25e-01	2022	0.489	
C - E	4.12e-02	1.19e-01	2023	0.986	
C - I	1.34e-01	1.25e-01	2023	0.711	
C - L	1.87e-01	1.19e-01	2023	0.4	
E - I	9.24e-02	1.25e-01	2023	0.882	
E - L	1.46e-01	1.19e-01	2023	0.612	
I - L	5.39e-02	1.25e-01	2023	0.973	
<b>C - E</b>	<b>-4.66E-01</b>	<b>1.19e-01</b>	<b>2024</b>	<b>0.001</b>	***
C - I	-1.05E-01	1.25e-01	2024	0.837	
<i>C - L</i>	<i>-3.10E-01</i>	<i>1.19e-01</i>	<i>2024</i>	<i>0.051</i>	+
<b>E - I</b>	<b>3.61e-01</b>	<b>1.25e-01</b>	<b>2024</b>	<b>0.024</b>	*
E - L	1.56e-01	1.19e-01	2024	0.559	
I - L	-2.05E-01	1.25e-01	2024	0.363	

Table S10) Section-level RWI - Location 2 (Adventdalen, Polygonal Tundra), 2022-2024.  
Type III Analysis of Variance Table with Kenward-Roger's method.

<b>term</b>	<b>sumsq</b>	<b>meansq</b>	<b>NumDF</b>	<b>DenDF</b>	<b>F value</b>	<b>p value</b>
<i>Treatment</i>	0.952	0.317	3	58	2.372	0.08
Year	0.415	0.208	2	116	1.552	0.216
Section	0.085	0.042	2	58	0.316	0.73
Treatment:Year	0.846	0.141	6	116	1.053	0.395
Treatment:Section	0.418	0.07	6	58	0.52	0.791
Year:Section	0.303	0.076	4	116	0.567	0.687
Treatment:Year:Section	1.482	0.124	12	116	0.923	0.527

Table S11) Section-level RWI - Location 5 (Ny-Alesund, Westbyelva), 2022-2024. Type III Analysis of Variance Table with Kenward-Roger's method.

<b>term</b>	<b>sumsq</b>	<b>meansq</b>	<b>NumDF</b>	<b>DenDF</b>	<b>F value</b>	<b>p value</b>
Treatment	0.454	0.151	3	57	1.166	0.331
<b>Year</b>	<b>5.293</b>	<b>2.647</b>	<b>2</b>	<b>114</b>	<b>20.412</b>	<b>2.65E<sup>-8</sup></b>
<i>Section</i>	0.652	0.326	2	57	2.514	0.09
<b>Treatment:Year</b>	<b>2.908</b>	<b>0.485</b>	<b>6</b>	<b>114</b>	<b>3.739</b>	<b>0.002</b>
Treatment:Section	0.255	0.042	6	57	0.328	0.92
Year:Section	0.711	0.178	4	114	1.371	0.248
Treatment:Year:Section	1.425	0.119	12	114	0.916	0.534



**Figure S8)** Ring-Width Index (RWI) per treatment per section type over the common period 2022-2024 for **a)** Location 2 (Adventdalen, Polygonal Tundra) and **b)** 5 (Ny-Alesund, Westbyelva). Jittered dots indicate shrub-averaged RWI, vertical lines indicate the estimated 95% confidence interval (CI) per treatment per year. Columns indicate years, rows indicate sections (R = root, C = root collar, S = shoot). No significant pairwise contrasts are indicated since none were found (Table S10, S11).

## References

- Ackerman, D., Griffin, D., Hobbie, S. E. & Finlay, J. C. (2017) Arctic shrub growth trajectories differ across soil moisture levels. *Global Change Biology*, **23**, 4294-4302. <https://doi.org/10.1111/gcb.13677>.
- AMAP (2021) Arctic Climate Change Update 2021: Key Trends and Impacts. Summary for Policy-makers. pp. 16 pp. Tromsø, Norway. ISBN – 978-82-7971-201-5.
- AMAP (2025) Arctic Climate Change Update 2024: Key Trends and Impacts. Summary for Policy-makers. . pp. 16 pp.
- Andersen, E. K., Dwinnell, S. P., Loe, L. E., Iveland, C. & van der Wal, R. (2025) Waterlogging of soil induces diverging rates of senescence in Svalbard reindeer forage plants. *Arctic, Antarctic, and Alpine Research*, **57**, 2441002. <https://doi.org/10.1080/15230430.2024.2441002>.
- Bates, D., Maechler, M., Bolker, B., Walker, S., Christensen, R. H. B., Singmann, H., Dai, B., Grothendieck, G., Green, P. & Bolker, M. B. (2024) Package 'lme4'. *version*, **12**, 2. <https://doi.org/10.32614/CRAN.package.lme4>.
- Berner, L. T., Massey, R., Jantz, P., Forbes, B. C., Macias-Fauria, M., Myers-Smith, I., Kumpula, T., Gauthier, G., Andreu-Hayles, L., Gaglioti, B. V., Burns, P., Zetterberg, P., D'Arrigo, R. & Goetz, S. J. (2020) Summer warming explains widespread but not uniform greening in the Arctic tundra biome. *Nature Communications*, **11**. <https://doi.org/10.1038/s41467-020-18479-5>.
- Bintanja, R. & Andry, O. (2017) Towards a rain-dominated Arctic. *Nature Climate Change*, **7**, 263-267. <https://doi.org/10.1038/nclimate3240>.
- Bintanja, R., van der Wiel, K., Van der Linden, E., Reusen, J., Bogerd, L., Krikken, F. & Selten, F. (2020) Strong future increases in Arctic precipitation variability linked to poleward moisture transport. *Science advances*, **6**, eaax6869. <https://doi.org/10.1126/sciadv.aax6869>.
- Biondi, F. & Qeadan, F. (2008) A theory-driven approach to tree-ring standardization: defining the biological trend from expected basal area increment. *Tree-Ring Research*, **64**, 81-96.
- Bjorkman, A. D., Myers-Smith, I. H., Elmendorf, S. C., Normand, S., Ruger, N., Beck, P. S. A., Blach-Overgaard, A., Blok, D., Cornelissen, J. H. C., Forbes, B. C., Georges, D., Goetz, S. J., Guay, K. C., Henry, G. H. R., HilleRisLambers, J., Hollister, R. D., Karger, D. N., Kattge, J., Manning, P., Prevey, J. S., Rixen, C., Schaepman-Strub, G., Thomas, H. J. D., Vellend, M., Wilmking, M., Wipf, S., Carboognani, M., Hermanutz, L., Levesque, E., Molau, U., Petraglia, A., Soudzilovskaia, N. A., Spasojevic, M. J., Tomaselli, M., Vowles, T., Alatalo, J. M., Alexander, H. D., Anadon-Rosell, A., Angers-Blondin, S., te Beest, M., Berner, L., Bjork, R. G., Buchwal, A., Buras, A., Christie, K., Cooper, E. J., Dullinger, S., Elberling, B., Eskelinen, A., Frei, E. R., Grau, O., Grogan, P., Hallinger, M., Harper, K. A., Heijmans, M., Hudson, J., Hulber, K., Iturrate-Garcia, M., Iversen, C. M., Jaroszynska, F., Johnstone, J. F., Jorgensen, R. H., Kaarlejarvi, E., Klady, R., Kuleza, S., Kulonen, A., Lamarque, L. J., Lantz, T., Little, C. J., Speed, J. D. M., Michelsen, A., Milbau, A., Nabe-Nielsen, J., Nielsen, S. S., Ninot, J. M., Oberbauer, S. F., Olofsson, J., Onipchenko, V. G., Rumpf, S. B., Semenchuk, P., Shetti, R., Collier, L. S., Street, L. E., Suding, K. N., Tape, K. D., Trant, A., Treier, U. A., Tremblay, J. P., Tremblay, M., Venn, S., Weijers, S., Zamin, T., Boulanger-Lapointe, N., Gould, W. A., Hik, D. S., Hofgaard, A., Jonsdottir, I. S., Jorgenson, J., Klein, J., Magnusson, B., et al. (2018) Plant functional trait change across a warming tundra biome. *Nature*, **562**, 57-+. <https://doi.org/10.1038/s41586-018-0563-7>.
- Bjørkvoll, E., Pedersen, B., Hytteborn, H., Jónsdóttir, I. S. & Langvatn, R. (2009) Seasonal and Interannual Dietary Variation During Winter in Female Svalbard Reindeer (*Rangifer Tarandus Platyrhynchus*). *Arctic, Antarctic, and Alpine Research*, **41**, 88-96. [10.1657/1523-0430-41.1.88](https://doi.org/10.1657/1523-0430-41.1.88).

- Blok, D., Sass-Klaassen, U., Schaepman-Strub, G., Heijmans, M., Sauren, P. & Berendse, F. (2011) What are the main climate drivers for shrub growth in Northeastern Siberian tundra? *Biogeosciences*, **8**, 1169-1179. <https://doi.org/10.5194/bg-8-1169-2011>.
- Briffa, K. & Jones, P. (1990) Basic chronology statistics and assessment. *Methods of dendrochronology*.
- Buchwal, A., Rachlewicz, G., Fonti, P., Cherubini, P. & Gärtner, H. (2013) Temperature modulates intra-plant growth of *Salix polaris* from a high Arctic site (Svalbard). *Polar Biology*, **36**, 1305-1318.
- Buchwal, A., Sullivan, P. F., Macias-Fauria, M., Post, E., Myers-Smith, I. H., Stroeve, J. C., Blok, D., Tape, K. D., Forbes, B. C. & Ropars, P. (2020) Divergence of Arctic shrub growth associated with sea ice decline. *Proceedings of the National Academy of Sciences*, **117**, 33334-33344. <https://doi.org/10.1073/pnas.2013311117>.
- Bunn, A. G. (2008) A dendrochronology program library in R (dplR). *Dendrochronologia*, **26**, 115-124.
- CAVMTeam (2003) Circumpolar Arctic Vegetation. US Fish and Wildlife Service. <https://arcticatlas.geobotany.org/catalog/dataset/circumpolar-arctic-vegetation-map-cavm-team-2003>.
- Chen, D., Fu, C., Jenkins, L. K., He, J., Wang, Z., Jandt, R. R., Frost, G. V., Bredder, A., Berner, L. T. & Loboda, T. V. (2024) Regional fire–greening positive feedback loops in Alaskan Arctic tundra. *Nature Plants*, 1-6.
- Cook, E., Briffa, K., Shiyatov, S. & Mazepa, V. (1990) Tree-ring standardization and growth-trend estimation. In Cook, ER and Kairiukstis, LA (Eds). *Methods of Dendrochronology: Applications in the Environmental Sciences*. Kluwer Academic Publishers, Dordrecht.
- Cook, E. R. & Kairiukstis, L. (1990) *Methods of Dendrochronology*. Kluwer Academic, Dordrecht.
- Dou, T., Pan, S., Bintanja, R. & Xiao, C. (2022) More frequent, intense, and extensive rainfall events in a strongly warming Arctic. *Earth's Future*, **10**, e2021EF002378. <https://doi.org/10.1029/2021EF002378>.
- Elmendorf, S. C., Henry, G. H., Hollister, R. D., Björk, R. G., Boulanger-Lapointe, N., Cooper, E. J., Cornelissen, J. H., Day, T. A., Dorrepaal, E., Elumeeva, T. G., Gill, M., Gould, W. A., Harte, J., Hik, D. S., Hofgaard, A., Johnson, D. R., Johnstone, J. F., Jónsdóttir, I. S., Jorgenson, J. C., Klanderud, K., Klein, J. A., Koh, S., Kudo, G., Lara, M., Lévesque, E., Magnússon, B., May, J. L., Mercado-Díaz, J. A., Michelsen, A., Molau, U., Myers-Smith, I. H., Oberbauer, S. F., Onipchenko, V. G., Rixen, C., Schmidt, N. M., Shaver, G. R., Spasojevic, M. J., Þórhallsdóttir, Þ. E., Tolvanen, A., Troxler, T., Tweedie, C. E., Villareal, S., Wahren, C.-H., Walker, X., Webber, P. J., Welker, J. M. & Wipf, S. (2012a) Plot-scale evidence of tundra vegetation change and links to recent summer warming. *Nature Climate Change*, **2**, 453-457. <https://doi.org/10.1038/nclimate1465>.
- Elmendorf, S. C., Henry, G. H. R., Hollister, R. D., Björk, R. G., Bjorkman, A. D., Callaghan, T. V., Collier, L. S., Cooper, E. J., Cornelissen, J. H. C., Day, T. A., Fosaa, A. M., Gould, W. A., Grétarsdóttir, J., Harte, J., Hermanutz, L., Hik, D. S., Hofgaard, A., Jarrad, F., Jónsdóttir, I. S., Keuper, F., Klanderud, K., Klein, J. A., Koh, S., Kudo, G., Lang, S. I., Loewen, V., May, J. L., Mercado, J., Michelsen, A., Molau, U., Myers-Smith, I. H., Oberbauer, S. F., Pieper, S., Post, E., Rixen, C., Robinson, C. H., Schmidt, N. M., Shaver, G. R., Stenström, A., Tolvanen, A., Totland, Ø., Troxler, T., Wahren, C.-H., Webber, P. J., Welker, J. M. & Wookey, P. A. (2012b) Global assessment of experimental climate warming on tundra vegetation: heterogeneity over space and time. *Ecology Letters*, **15**, 164-175. <https://doi.org/10.1111/j.1461-0248.2011.01716.x>.
- Elvebakk, A. (1999) Bioclimatic delimitation and subdivision of the Arctic. *The Species Concept in the High North—A Panarctic Flora Initiative*, 81-112.

- Elven, R., Arnesen, G., Alsos, I. & Sandbakk, B. (2020) Svalbardflora - Vascular plants in Svalbard. [www.svalbardflora.no](http://www.svalbardflora.no) [accessed April 2025].
- Fauchald, P., Park, T., Tømmervik, H., Myneni, R. & Hausner, V. H. (2017) Arctic greening from warming promotes declines in caribou populations. *Science Advances*, **3**, e1601365.
- Francon, L., Corona, C., Till-Bottraud, I., Choler, P., Carlson, B., Charrier, G., Améglio, T., Morin, S., Eckert, N. & Roussel, E. (2020) Assessing the effects of earlier snow melt-out on Alpine shrub growth: the sooner the better? *Ecological Indicators*, **115**, 106455.
- Frost, G. V., Bhatt, U. S., Macander, M. J., Berner, L. T., Walker, D. A., Reynolds, M. K., Magnússon, R. Í., Bartsch, A., Bjerke, J. W., Epstein, H. E., Forbes, B. C., Goetz, S. J., Hoy, E. E., Karlsen, S. R., Kumpula, T., Lantz, T. C., Lara, M. J., López-Blanco, E., Montesano, P. M., Neigh, C. S. R., Nitze, I., Orndahl, K. M., Park, T., Phoenix, G. K., Rocha, A. V., Rogers, B. M., Schaepman-Strub, G., Tømmervik, H., Verdonen, M., Veremeeva, A., Virkkala, A.-M. & Waigl, C. F. (2025) The changing face of the Arctic: four decades of greening and implications for tundra ecosystems. *Frontiers in Environmental Science*, **Volume 13 - 2025**. 10.3389/fenvs.2025.1525574.
- Gamm, C. M., Sullivan, P. F., Buchwal, A., Dial, R. J., Young, A. B., Watts, D. A., Cahoon, S. M. P., Welker, J. M. & Post, E. (2018) Declining growth of deciduous shrubs in the warming climate of continental western Greenland. *Journal of Ecology*, **106**, 640-654. <https://doi.org/10.1111/1365-2745.12882>.
- Gärtner, H., Lucchinetti, S. & Schweingruber, F. H. (2014) New perspectives for wood anatomical analysis in dendrosciences: the GSL1-microtome. *Dendrochronologia*, **32**, 47-51.
- Gärtner, H. & Schweingruber, F. (2013) *Microscopic preparation techniques for plant stem analysis*. Verlag Dr. Kessel, Remagen-Oberwinter.
- Hallinger, M., Manthey, M. & Wilmking, M. (2010) Establishing a missing link: warm summers and winter snow cover promote shrub expansion into alpine tundra in Scandinavia. *New Phytologist*, **186**, 890-899.
- Hanssen-Bauer, I., Førland, E., Hisdal, H., Mayer, S., Sandø, A. B. & Sorteberg, A. (2019) Climate in Svalbard 2100. *A knowledge base for climate adaptation*, **470**. NCCS report no. 1/2019.
- Heijmans, M. M., Magnússon, R. Í., Lara, M. J., Frost, G. V., Myers-Smith, I. H., van Huissteden, J., Jorgenson, M. T., Fedorov, A. N., Epstein, H. E. & Lawrence, D. M. (2022) Tundra vegetation change and impacts on permafrost. *Nature Reviews Earth & Environment*, **3**, 68-84. <https://doi.org/10.1038/s43017-021-00233-0>.
- Henry, G. H., Hollister, R. D., Klanderud, K., Björk, R. G., Bjorkman, A. D., Elphinstone, C., Jónsdóttir, I. S., Molau, U., Petraglia, A. & Oberbauer, S. F. (2022) The International Tundra Experiment (ITEX): 30 years of research on tundra ecosystems. *Arctic Science*, **8**, 550-571. <https://doi.org/10.1139/as-2022-0041>.
- Iturrate-Garcia, M., Heijmans, M. M., Schweingruber, F. H., Maximov, T. C., Niklaus, P. A. & Schaepman-Strub, G. (2017) Shrub growth rate and bark responses to soil warming and nutrient addition—A dendroecological approach in a field experiment. *Dendrochronologia*, **45**, 12-22.
- Karlsen, S. R., Elvebakk, A., Stendardi, L., Høgda, K. A. & Macias-Fauria, M. (2024) Greening of Svalbard. *Science of the Total Environment*, **945**, 174130. <https://doi.org/10.1016/j.scitotenv.2024.174130>.
- Keuper, F., Parmentier, F.-J. W., Blok, D., van Bodegom, P. M., Dorrepaal, E., van Hal, J. R., van Logtestijn, R. S. & Aerts, R. (2012) Tundra in the rain: differential vegetation responses to three years of experimentally doubled summer precipitation in Siberian shrub and Swedish bog tundra. *Ambio*, **41**, 269-280. <https://doi.org/10.1007/s13280-012-0305-2>.
- Kolischuk, V. G. (1990) Dendroclimatological Study of Prostrate Woody Plants. *Methods of Dendrochronology: Applications in the Environmental Sciences* (ed E. Cook, Kairiukstis, L). Kluwer Academic Publishers, Dordrecht.

- Kuznetsova, A., Brockhoff, P. B. & Christensen, R. H. B. (2024) Package 'lmerTest'. *R package version, 1.10.5*. <https://doi.org/10.32614/CRAN.package.lmerTest>.
- Le Moullec, M., Buchwal, A., van der Wal, R., Sandal, L. & Hansen, B. B. (2019) Annual ring growth of a widespread high arctic shrub reflects past fluctuations in community-level plant biomass. *Journal of Ecology*, **107**, 436-451. <https://doi.org/10.1111/1365-2745.13036>.
- Le Moullec, M., Sandal, L., Grøtan, V., Buchwal, A. & Hansen, B. B. (2020) Climate synchronises shrub growth across a high-arctic archipelago: contrasting implications of summer and winter warming. *Oikos*, **129**, 1012-1027.
- Lenth, R. V. (2024) Package 'emmeans'. *R package version*. <https://doi.org/10.32614/CRAN.package.emmeans>.
- Li, B., Heijmans, M. M., Berendse, F., Blok, D., Maximov, T. & Sass-Klaassen, U. (2016) The role of summer precipitation and summer temperature in establishment and growth of dwarf shrub *Betula nana* in northeast Siberian tundra. *Polar Biology*, **39**, 1245-1255.
- Loranty, M. M., Abbott, B. W., Blok, D., Douglas, T. A., Epstein, H. E., Forbes, B. C., Jones, B. M., Kholodov, A. L., Kropp, H. & Malhotra, A. (2018) Reviews and syntheses: Changing ecosystem influences on soil thermal regimes in northern high-latitude permafrost regions. *Biogeosciences*, **15**, 5287-5313. <https://doi.org/10.5194/bg-15-5287-2018>.
- Magnússon, R., Schuur, S., Hamm, A., Verhoeven, M., Limpens, J., Loonen, M. & Lang, S. I. (2024) Limited sensitivity of permafrost soils to heavy rainfall across Svalbard ecosystems. *Science of the Total Environment*, 173696. <https://doi.org/10.1016/j.scitotenv.2024.173696>.
- Magnússon, R. Í., Sass-Klaassen, U., Limpens, J., Karsanaev, S. V., Ras, S., van Huissteden, K., Blok, D. & Heijmans, M. M. (2023) Spatiotemporal variability in precipitation-growth association of *Betula nana* in the Siberian lowland tundra. *Journal of Ecology*, **111**, 1882-1904. <https://doi.org/10.1111/1365-2745.14165>.
- Mekonnen, Z. A., Riley, W. J., Berner, L. T., Bouskill, N. J., Torn, M. S., Iwahana, G., Breen, A. L., Myers-Smith, I. H., Criado, M. G. & Liu, Y. (2021) Arctic tundra shrubification: a review of mechanisms and impacts on ecosystem carbon balance. *Environmental Research Letters*, **16**, 053001.
- Melvin, T. (2004) *Historical growth rates and changing climatic sensitivity of boreal conifers*. University of East Anglia.
- Myers-Smith, I. H., Elmendorf, S. C., Beck, P. S., Wilms, M., Hallinger, M., Blok, D., Tape, K. D., Rayback, S. A., Macias-Fauria, M. & Forbes, B. C. (2015a) Climate sensitivity of shrub growth across the tundra biome. *Nature Climate Change*, **5**, 887. <https://doi.org/10.1038/nclimate2697>.
- Myers-Smith, I. H., Grabowski, M. M., Thomas, H. J. D., Angers-Blondin, S., Daskalova, G. N., Bjorkman, A. D., Cunliffe, A. M., Assmann, J. J., Boyle, J. S., McLeod, E., McLeod, S., Joe, R., Lennie, P., Arey, D., Gordon, R. R. & Eckert, C. D. (2019) Eighteen years of ecological monitoring reveals multiple lines of evidence for tundra vegetation change. *Ecological Monographs*, **89**. 10.1002/ecm.1351.
- Myers-Smith, I. H., Hallinger, M., Blok, D., Sass-Klaassen, U., Rayback, S. A., Weijers, S., Trant, A. J., Tape, K. D., Naito, A. T. & Wipf, S. (2015b) Methods for measuring arctic and alpine shrub growth: a review. *Earth-Science Reviews*, **140**, 1-13.
- Nakatsubo, T., Fujiyoshi, M., Yoshitake, S., Koizumi, H. & Uchida, M. (2010) Colonization of the polar willow *Salix polaris* on the early stage of succession after glacier retreat in the High Arctic, Ny-Ålesund, Svalbard. *Polar research*, **29**, 285-390.
- NCCS (2025) SEKLIMA. Norwegian Centre for Climate Services. <https://seklima.met.no/> [accessed March 2025].
- Nordli, Ø., Wyszynski, P., Gjelten, H., Isaksen, K., Łupikasza, E., Niedźwiedz, T. & Przybylak, R. (2020) Revisiting the extended Svalbard Airport monthly temperature series, and the compiled corresponding daily series 1898–2018. <http://dx.doi.org/10.33265/polar.v39.3614>.

- Opala-Owczarek, M., Pirożnikow, E., Owczarek, P., Szymański, W., Luks, B., Kępski, D., Szymanowski, M., Wojtuń, B. & Migala, K. (2018) The influence of abiotic factors on the growth of two vascular plant species (*Saxifraga oppositifolia* and *Salix polaris*) in the High Arctic. *Catena*, **163**, 219-232. <https://doi.org/10.1016/j.catena.2017.12.018>.
- Owczarek, P. & Opala-Owczarek, M. (2016) Dendrochronology and extreme pointer years in the tree-ring record (AD 1951-2011) of polar willow from southwestern Spitsbergen (Svalbard, Norway).
- Owczarek, P., Opala-Owczarek, M. & Migala, K. (2020) Post-1980s shift in the sensitivity of tundra vegetation to climate revealed by the first dendrochronological record from Bear Island (Bjørnøya), western Barents Sea. *Environmental Research Letters*, **16**, 014031.
- Peeters, B., Pedersen, Å. Ø., Loe, L. E., Isaksen, K., Veiberg, V., Stien, A., Kohler, J., Gallet, J.-C., Aanes, R. & Hansen, B. B. (2019) Spatiotemporal patterns of rain-on-snow and basal ice in high Arctic Svalbard: detection of a climate-cryosphere regime shift. *Environmental Research Letters*, **14**, 015002.
- Power, C. C., Normand, S., von Arx, G., Elberling, B., Corcoran, D., Krog, A. B., Bouvin, N. K., Treier, U. A., Westergaard-Nielsen, A. & Liu, Y. (2024) No effect of snow on shrub xylem traits: Insights from a snow-manipulation experiment on Disko Island, Greenland. *Science of the Total Environment*, **916**, 169896.
- Prevéy, J. S., Rixen, C., Rüger, N., Høye, T. T., Bjorkman, A. D., Myers-Smith, I. H., Elmendorf, S. C., Ashton, I. W., Cannone, N. & Chisholm, C. L. (2019) Warming shortens flowering seasons of tundra plant communities. *Nature ecology & evolution*, **3**, 45-52. <https://doi.org/10.1038/s41559-018-0745-6>.
- Rantanen, M., Karpechko, A. Y., Lipponen, A., Nordling, K., Hyvärinen, O., Ruosteenoja, K., Vihma, T. & Laaksonen, A. (2022) The Arctic has warmed nearly four times faster than the globe since 1979. *Communications Earth & Environment*, **3**, 168. <https://doi.org/10.1038/s43247-022-00498-3>.
- Schuur, E. A., Abbott, B. W., Commane, R., Ernakovich, J., Euskirchen, E., Hugelius, G., Grosse, G., Jones, M., Koven, C. & Leshyk, V. (2022) Permafrost and climate change: carbon cycle feedbacks from the warming Arctic. *Annual Review of Environment and Resources*, **47**, 343-371.
- See, C. R., Virkkala, A.-M., Natali, S. M., Rogers, B. M., Mauritz, M., Biasi, C., Bokhorst, S., Boike, J., Bret-Harte, M. S. & Celis, G. (2024) Decadal increases in carbon uptake offset by respiratory losses across northern permafrost ecosystems. *Nature Climate Change*, **14**, 853-862.
- Strand, S. M., Christiansen, H. H., Johansson, M., Åkerman, J. & Humlum, O. (2021) Active layer thickening and controls on interannual variability in the Nordic Arctic compared to the circum-Arctic. *Permafrost and Periglacial Processes*, **32**, 47-58.
- Tei, S., Sugimoto, A., Kotani, A., Ohta, T., Morozumi, T., Saito, S., Hashiguchi, S. & Maximov, T. (2019) Strong and stable relationships between tree-ring parameters and forest-level carbon fluxes in a Siberian larch forest. *Polar Science*, **21**, 146-157. <https://doi.org/10.1016/j.polar.2019.02.001>.
- van den Broek, D., Urbancic, G. H., Rantanen, M. & Vihma, T. (2025) Svalbard's record-breaking arctic summer 2024: Anomalies beyond climatological warming trends. *Geophysical Research Letters*, **52**, e2025GL115015.
- Vickers, H., Malnes, E. & Eckerstorfer, M. (2022) A synthetic aperture radar based method for long term monitoring of seasonal snowmelt and wintertime rain-on-snow events in Svalbard. *Frontiers in Earth Science*, **10**, 868945.
- Wang, P., Huang, Q., Tang, Q., Chen, X., Yu, J., Pozdniakov, S. P. & Wang, T. (2021) Increasing annual and extreme precipitation in permafrost-dominated Siberia during 1959–2018. *Journal of Hydrology*, **603**, 126865. <https://doi.org/10.1016/j.jhydrol.2021.126865>.
- Wilmking, M., Hallinger, M., Van Bogaert, R., Kyncl, T., Babst, F., Hahne, W., Juday, G., De Luis, M., Novak, K. & Völlm, C. (2012) Continuously missing outer rings in woody plants at their distributional margins. *Dendrochronologia*, **30**, 213-222.

Zang, C. & Biondi, F. (2015) treeclim: an R package for the numerical calibration of proxy-climate relationships. *Ecography*, **38**, 431-436.